
ON THE INTERCONNECTIONS OF CALIBRATION, QUANTIFICATION, AND CLASSIFIER ACCURACY PREDICTION UNDER DATASET SHIFT

Alejandro Moreo

Istituto di Scienza e Tecnologie dell'Informazione, Consiglio Nazionale delle Ricerche
Via Giuseppe Moruzzi 1, 56124, Pisa, Italy
alejandro.moreo@isti.cnr.it

ABSTRACT

When the distribution of the data used to train a classifier differs from that of the test data, i.e., under dataset shift, well-established routines for calibrating the decision scores of the classifier, estimating the proportion of positives in a test sample, or estimating the accuracy of the classifier, become particularly challenging. This paper investigates the interconnections among three fundamental problems, calibration, quantification, and classifier accuracy prediction, under dataset shift conditions. Specifically, we prove their equivalence through mutual reduction, i.e., we show that access to an oracle for any one of these tasks enables the resolution of the other two. Based on these proofs, we propose new methods for each problem based on direct adaptations of well-established methods borrowed from the other disciplines. Our results show such methods are often competitive, and sometimes even surpass the performance of dedicated approaches from each discipline. The main goal of this paper is to fostering cross-fertilization among these research areas, encouraging the development of unified approaches and promoting synergies across the fields.

Keywords dataset shift · classifier calibration · quantification · classifier accuracy prediction

1 Introduction

Classifiers are often deployed in contexts in which the *independent and identically distributed* (IID) assumption is violated, i.e., in which the data used to train the model and the future data to be classified are not drawn from the same distribution. This situation is generally referred to as *dataset shift* in the machine learning literature [Storkey, 2009].

In this context, three problems have gained increased attention in the last years. *Classifier calibration* [Flach and Webb, 2016, Silva Filho et al., 2023] concerns the manipulation of the confidence scores produced by a classifier so that these effectively reflect the likelihood that a given instance is positive. *Quantification* [González et al., 2017, Esuli et al., 2023] is instead concerned with estimating the prevalence of the classes of interest in an unlabelled set. Finally, *classifier accuracy prediction* aims at inferring how well a classifier will fare on unseen data [Elsahar and Gallé, 2019, Guillory et al., 2021].

Well-established procedures for attaining these three goals when the IID assumption holds are known and routinely used. For instance, calibrating the classifier's outputs can be attained by learning a calibration map (a function mapping classifier confidence scores into values reflecting the likelihood of the positive class) on held-out validation data [Platt, 2000, Zadrozny and Elkan, 2001a, Barlow and Brunk, 1972].¹ Concerning quantification, the class proportions in a test set can be estimated by simply classifying and counting how many positives fall under which class. Finally, the performance that a classifier will exhibit on unseen data can be estimated on held-out validation data [Hastie et al., 2009].

¹Notwithstanding this, calibration under IID conditions is still an active area of research; see, e.g., [Tasche, 2021].

However, when the IID assumption is violated, these standard routines are prone to failure. For example, calibration is a property typically defined with respect to a specific distribution, meaning that a classifier is unlikely to remain well-calibrated across different distributions [Ovadia et al., 2019]. Similarly, the commonly used “classify and count” approach for class prevalence estimation is known to yield biased predictions under certain dataset shift conditions [Esuli et al., 2023, §1.2]. Likewise, the accuracy of a classifier estimated on held-out validation data or via cross-validation is biased when the IID assumption does not hold [Storkey, 2009].

The three problems are deeply interconnected and may arise in related real-world applications. Consider, for example, a classifier trained on X-ray lung images to assist clinical decisions regarding medical interventions. In order for the classifier to aid in making informed decisions, the classifier must not only provide classifier decisions, but also a measure of uncertainty attached to it, i.e., its outputs must be well calibrated. Now, suppose a pandemic occurs, altering the natural prevalence of a pneumonic virus in the population. In response, several actions must be undertaken to develop a trustworthy response to the virus. Estimating the prevalence of the population affected by the virus (for which any of the quantification methods discussed in [González et al., 2017] can be employed) is of the utmost importance for epidemiologists [Patrone and Kearsley, 2024]; these prevalence estimates are useful to recalibrate the classifier outputs to reflect the new priors [Godau et al., 2025] (using techniques such as those in [Elkan, 2001, Guilbert et al., 2024]). Alternatively, the practitioner might need to estimate the accuracy of different candidate classifiers under the new conditions in order to, e.g., replace the existing classifier with a different one that is expected to perform more accurately in the new distribution, or maybe to reweigh the relative importance of different classifiers in an ensemble (which necessitate methods for classifier accuracy prediction such as, e.g., [Guillory et al., 2021, Garg et al., 2022]). A better understanding of the interdependencies between the three problems may lead to more robust and integrated solutions, especially in dynamic or high-stakes environments such as healthcare.

However, the applicability of one technique or another is ultimately subject to verifying certain assumptions about the relationship between the underlying distributions. In the context of dataset shift [Storkey, 2009], the two most important such types of shift include *covariate shift* (CS) and *prior probability shift* (aka *label shift* –LS). CS presupposes a change in the marginal distribution of the observed features, while the posterior probabilities are assumed stationary. Conversely, LS has to do with a change in the class prevalence subject to stationary class-conditional distributions of the observed features. More formal definitions are provided later on.

In this paper, we argue that the interplay between the three problems is deeper than it seems at first glance. We begin by offering formal proofs of their equivalence via reduction, showing that having access to a perfect model (an oracle) for any of these problems will automatically enable the resolution of the other two tasks. We then build on those formalizations to propose practical adaptations of methods from each discipline to address the other two. Somehow surprisingly, our results show that some of these adaptations tend to perform unexpectedly well in other problems. The main contribution of this paper is to raise awareness of the close relationship between these problems, with the hope of fostering cross-fertilization among different fields and promoting unified solutions.

The rest of this paper is structured as follows. In Section 2 we review some occasional interactions among calibration, quantification, and classifier accuracy prediction in the literature, as well as dedicated related work for each discipline. Section 3 is devoted to fix the notation and present technical definitions which are functional to the proofs of problems equivalence via reduction presented in Section 4. Section 5 explores new methods that we propose for each of the three task, by adapting principles and techniques borrowed from the other tasks. We report the experiments we have carried out in Section 6, in which we confront proper methods from each discipline with the newly proposed adaptations. Section 7 offers some final discussions and wraps up, while also suggesting potential ideas for future work.

2 Related Work

Perhaps the most obvious link between the three problems pivots on classifier calibration. Despite the fact that the frequent co-occurrence of the term “calibration” with the term “quantification” in the literature often actually refers to “uncertainty quantification”, and not to “quantification” in the sense of class prevalence estimation, it is a well-known fact in the quantification community that a properly calibrated classifier for the test distribution would automatically enable an accurate estimator of class prevalence [Card and Smith, 2018, Tasche, 2014]. Conversely, the link between calibration and classifier accuracy prediction is embedded in the definition of the calibration property itself, according to which the predicted confidence of a perfectly calibrated classifier is a good approximation of its actual *probability of correctness* [Silva Filho et al., 2023, Chen and Su, 2023].

Beyond this, some sporadic interconnections among the problems have been echoed recently in [Wu and Resnick, 2024], in which quantification and calibration take part in the so-called “Calibrate-Extrapolate” framework for applications in the social sciences; and in [Volpi et al., 2024], in which quantification is used to support the task of classifier accuracy prediction.

The remainder of this section reviews the related literature on calibration (Section 2.1), quantification (Section 2.2), and classifier accuracy prediction (Section 2.3).

2.1 Calibration

The concept of model calibration first appeared in the field of meteorology [Murphy, 1972], and is nowadays used to refer to techniques for transforming the confidence scores generated by a classifier into estimates of posterior probabilities, i.e., into values reflecting the probability of a datapoint to belong to each class of interest [Flach and Webb, 2016, Silva Filho et al., 2023]. A perfectly calibrated classifier is thus a model that perfectly accounts for its own uncertainty. For example, if a perfectly calibrated binary classifier returns 0.95 as the posterior probability for the positive class, we know that the classifier is confident that the instance is positive, but there is still 5% chance the decision is incorrect. Similarly, if the classifier returns 0.49, the classifier is also telling us that it is highly uncertain about the decision, suggesting that one should be very cautious if any critical decision is to be taken based on such prediction.

Calibration techniques may be divided in two categories: regularization-based and post-hoc calibration techniques. Regularization-based techniques add a calibration-oriented factor to the loss the model optimizes at training time. These techniques have proven useful for calibrating the output of modern neural networks, which are otherwise known to be poorly calibrated and typically overconfident [Guo et al., 2017]. Popular such techniques include temperature scaling [Hinton, 2015], vector scaling [Guo et al., 2017], and Dirichlet calibration [Kull et al., 2019].

On the other side, post-hoc calibration techniques use held-out validation data to learn a calibration map that transforms the confidence scores of a previously trained model. A calibration map can be learned using non-parametric techniques such as empirical binning [Zadrozny and Elkan, 2001a] or isotonic calibration [Barlow and Brunk, 1972], or using parametric ones such as Platt scaling [Platt, 2000], which relies on the logistic function, or more recent methods relying on more flexible parametric functions such as the beta calibration [Kull et al., 2017]. In this paper, we will hereafter focus on post-hoc calibration techniques.

In high-stakes domains with non-stationary conditions, having well-calibrated outputs is of crucial importance, since these can be easily adapted to changes in the class prior or changes in the cost distribution [Silva Filho et al., 2023]. Unfortunately, the post-hoc calibration techniques discussed above have been found to fall short of producing reliable estimates of classifier uncertainty in the presence of dataset shift [Ovadia et al., 2019, Karandikar et al., 2021]. As a response, several post-hoc methods have recently been proposed in the literature to cope with the problem of dataset shift [Park et al., 2020, Wang et al., 2020, Chen and Su, 2023, Popordanoska et al., 2024]. All these methods operate under the same conditions, i.e., that all available labelled examples come from the training (or “source”) distribution, while all examples from the test (or “target”) distribution are devoid of labels.

[Park et al., 2020] proposes Calibrated Prediction with Covariate Shift (CPCS), a calibration method that minimizes an upper bound on the expected calibration error (ECE), which is derived following assumptions from CS. The method adopts principles from domain adaptation, and relies on importance weighting to correct for the shift between the training and test distributions, respectively. The importance weights take the form of a ratio $\frac{Q(x)}{P(x)}$, where P and Q are the density functions of the training and test distributions. As such weights are unknown, the authors propose to estimate them using a “source vs. target” discriminator, i.e., by taking the posterior probability of a logistic regression model trained to identify whether an instance comes from the test distribution (acting as the positive class) or instead from the training one (acting as the negative class), in a surrogate binary classification problem.

Later on, a method called Transferable Calibration (TransCal) [Wang et al., 2020] was proposed in response to a phenomenon observed under CS assumptions, in which the improvement in classifier accuracy through domain adaptation techniques comes at the expense of ECE in the target distribution. TransCal is a hyperparameter-free method that minimizes a new calibration measure called Importance Weighted Expected Calibration Error (IWECE) which manages to estimate the calibration error in the target domain under CS assumptions with lower bias and variance than CPCS.

The Head2Tails calibration model [Chen and Su, 2023] was later proposed as a means to counter the distribution shift that occurs when the classifier is trained in a close-to-balanced setting, but the data to be classified in deployment conditions instead follow a long-tailed class distribution, where few classes (the “heads”) gather most of the density whereas many classes (the “tails”) are severely imbalanced. Classifiers trained this way tend to be overconfident for the “head” classes. The method estimates the importance weights of datapoints in the “tail” classes to better calibrate their outputs by transferring knowledge from the “heads”. Somehow surprisingly, though, the authors describe such a setting as an instance of CS. While it is clear that a shift in the class proportions results in a shift of the marginal distributions of the covariates, we believe such a setting is more representative of LS instead, since only the priors of the classes have changed. Later on, two closely related calibration methods (called “polynomial positive” and “exponential”) are presented in [Guilbert et al., 2024] in the context of imbalanced binary classification problems. The

main goal is to improve the calibrated outcome for the minority class (which represents the interesting phenomenon, such as a rare illness) on the grounds that no action is typically undertaken for the majority class examples (e.g., on healthy individuals).

Recently, the method LasCal [Popordanoska et al., 2024] has been proposed to better calibrate classifiers under LS. The method adopts a temperature scaling strategy, and optimizes for the temperature parameter by minimizing a pointwise consistent ECE that roots on the LS assumptions.

2.2 Quantification

Quantification was proposed by [Forman, 2005] as the machine learning task of estimating the class prevalence values in unlabelled sets; see [González et al., 2017, Esuli et al., 2023] for overviews. For this reason, most of the quantification methods proposed so far have mainly focused on scenarios characteristic of LS, i.e., in cases in which the priors are expected to vary with respect to the training conditions; see [Schumacher et al., 2025, Esuli et al., 2022, Esuli et al., 2024] for evaluation campaigns. Prototypical applications of quantification span areas such as epidemiology [King and Lu, 2008], social sciences [Hopkins and King, 2010], ecological modeling [Beijbom et al., 2015], market research [Esuli and Sebastiani, 2010], and sentiment analysis [Moreo and Sebastiani, 2022]. Conversely, little attention in the quantification literature has been paid to CS, aside from some theoretical analysis [Tasche, 2022, Tasche, 2023] and few experimental evaluations [González et al., 2024, Esuli et al., 2024].

The IID approach to quantification comes down to training a classifier using supervised examples from the training distribution, and use it to issue label predictions for the test examples; the class prevalence values are simply obtained by counting the fraction of instances that fall under each class. This method, called “classify and count” (CC) is a biased estimator under LS conditions [Esuli et al., 2023, §1.2], and represents a weak baseline any proper quantification method is expected to beat. However, when the fractions are instead counted as the expected value of a well-calibrated probabilistic classifier, i.e., when using the “probabilistic classify and count” method (PCC) [Bella et al., 2010], the resulting estimates are known to be accurate under CS assumptions [Card and Smith, 2018, Tasche, 2022].

Arguably, the method “adjusted classify and count” (ACC) [Forman, 2008] is the simplest way to correct for the bias of CC under LS. ACC applies a linear correction to the CC estimate (denoted by \hat{p}^{CC}), by taking into account an estimate of the true positive rate (tpr) and false positive rate (fpr) of the classifier. Under LS conditions, the tpr and fpr are assumed stationary, so they can be estimated in hold-out validation data from the training distribution (see also Remark 1 in Section 3.2). The method was later rediscovered and popularized in the machine learning community under the name of Black-Box Shift Estimator (BBSE) by [Lipton et al., 2018]. The probabilistic counterpart, dubbed “probabilistic adjusted classify and count” (PACC) [Bella et al., 2010], consists of replacing the crisp count obtained via CC with the expected soft count obtained via PCC, and also using the estimates of the posterior probabilities returned by the probabilistic classifier (instead of the crisp ones) to obtain estimates for the tpr and fpr.

One of the most important families of approaches in the quantification literature is the so-called distribution matching (DM) [Forman, 2005]. DM approaches seek for the mixture parameter (the sought class prevalence values) that yields a mixture of the class-conditional distributions of the training datapoints which is closest to the distribution of the test datapoints, in terms of any given divergence measure. Different methods have been proposed in the literature relying on different mechanisms for representing the distributions, including histograms of posteriors [González-Castro et al., 2013, Pérez-Mon et al., 2025] or Fourier transformations of the features [Dussap et al., 2023], and different divergence measures, including the Hellinger Distance [González-Castro et al., 2013] or the Topsøe divergence [Maletzke et al., 2019], among others. One DM-based method which has demonstrated superior performance in recent evaluations is KDEy [Moreo et al., 2025], in which distributions are represented by means of kernel density estimates of the posteriors, and in which the Kullback-Leibler divergence is adopted as the divergence measure to minimize.

Some efforts have been recently paid trying to unify the most important quantification methods under a common DM-based framework [Firat, 2016, Garg et al., 2020, Bunse, 2022, Castaño et al., 2023]. While the above-discussed methods can be framed as specific instances of these frameworks, one notable exception is the Expectation-Maximization method proposed by [Saerens et al., 2002], typically referred to as EMQ (or SLD after the name of its proponents [Esuli et al., 2021]) in the quantification literature. This method precedes the field of quantification itself, and was indeed proposed for a different scope: updating the posterior probabilities of the test datapoints, as estimated by a probabilistic classifier that has been calibrated for the training distribution, to a target distribution in which the priors have changed. The method relies on a mutually recursive update of the priors and the posteriors, following the EM algorithm, until convergence. While the method was originally proposed as a means for recalibrating the outputs of a probabilistic classifier with respect to a new prior under LS, it has become very popular in quantification endeavours, in which we rather take, as the output of the algorithm, the last updated priors found by the method. This method is known

to behave extremely well, and several enhancements have been proposed in the machine learning literature, including further recalibration rounds [Alexandari et al., 2020] and regularized variants thereof [Azizzadenesheli et al., 2019].

2.3 Classifier Accuracy Prediction

The standard method for estimating the classifier accuracy on future data under the IID assumption is cross-validation [Hastie et al., 2009]. Recently, some methods have been proposed to operate under dataset shift conditions, such as the *Reverse Classification Accuracy* (RCA) [Elsahar and Gallé, 2019], which bases its prediction on the validation accuracy of another classifier trained on test data labelled by the target classifier; *Mandoline* [Chen et al., 2021b], relying on importance weighting and density estimation; or [Chen et al., 2021a], which relies instead on the agreement ratio of an ensemble of auxiliary models which is updated iteratively; *Generalisation Disagreement Equality* (GDE) [Jiang et al., 2022], which analyzes the degree of disagreement on IID data of identical neural architectures as a proxy of their accuracy on shifted data.

In this paper, we will take a closer look at three recent methods that have showcased superior performance in recent years: ATC [Garg et al., 2022], DoC [Guillory et al., 2021] and LEAP [Volpi et al., 2024].

ATC, standing for *Average Thresholded Confidence* [Garg et al., 2022], searches for the threshold value t on the confidence value of a classifier that yields, on validation data, a proportion of datapoints with confidence higher than it equals the proportion of datapoints correctly classified (i.e., equals the classifier accuracy score on the validation data). The authors proposed to compute the confidence value in terms of maximum confidence or negative entropy.

The method DoC, for *Difference of Confidence* [Guillory et al., 2021], learns a regression model to predict the model performance on the test set. The regressor is trained on a measure of distance between the in-distribution data and the out-of-distribution data. Such measure reflects the accuracy gap, and is computed in terms of the average max confidence over a series of validation samples V_i which are generated with the aim of reflecting the type of dataset shift to be faced. The underlying principle is that, if the model is well-calibrated and there is no shift, the expected value of the model’s confidence must coincide with its accuracy. The regressor is thus used to learn a correction from the average maximum confidence value to the actual accuracy under a shifted distribution.

Finally, LEAP (Linear Equation -based Accuracy Prediction) [Volpi et al., 2024] models the problem as a system of linear equations with n^2 unknowns, with n the number of classes. The equations are derived following the LS assumptions and relies, for their specification, on a quantification method (KDEy, see Section 2.2) as an intermediate step. A key difference of this method, is that it predicts the n^2 entries of a contingency table, and is thus not tied to one specific evaluation measure. While LEAP has proven to fare well under LS, it has never been tested under CS.

3 Preliminaries

This section introduces notation and definitions that will be instrumental for the following sections.

3.1 Notation

Let $\mathcal{X} \subset \mathbb{R}^d$ be the input space of the covariates for some $d \in \mathbb{N}$, and \mathcal{Y} be the output space of class labels. We will restrict our attention to the binary case, in which case we define $\mathcal{Y} = \{0, 1\}$ with 0 denoting the negative class, and 1 denoting the positive class. By \mathcal{S} we denote the space of samples of elements from \mathcal{X} .

We define a binary classifier as $h : \mathcal{X} \rightarrow \mathbb{R}$, i.e., as a function $h \in \mathcal{H}$, where \mathcal{H} denotes the class of hypotheses, returning raw (uncalibrated) confidence scores. From h we can obtain a crisp classifier $\tilde{h} : \mathcal{X} \rightarrow \mathcal{Y}$ via thresholding by simply defining $\tilde{h}(x) = 1$ if $h(x) > t$, and $\tilde{h}(x) = 0$ otherwise, for some threshold value $t \in \mathbb{R}$. We use $\tilde{h} : \mathcal{X} \rightarrow [0, 1]$ to denote a probabilistic classifier, i.e., a classifier whose outputs are interpretable as posterior probabilities.

We assume the classifier h has been generated using some training data $D_{tr} = \{(x_i, y_i)\}_{i=1}^m$, with $x_i \in \mathcal{X}, y_i \in \mathcal{Y}$. We also assume the existence of a test set $D_{te} = \{x_i\}_{i=1}^n$ for which we do not observe the true labels. We write $\Phi(x)$ to denote the true label of a test datapoint x . We assume a dataset shift scenario in which the training and test data have been drawn from two distributions P and Q , respectively, with $P \neq Q$. We use the random variables X, Y taking values, respectively, on \mathcal{X}, \mathcal{Y} . We will also use $\hat{Y} = \tilde{h}(X)$ and $\tilde{Y} = \tilde{h}(X)$ to denote the random variables of the classifier’s crisp and soft predictions, ranging on $\{0, 1\}$ and $[0, 1]$, respectively.

3.2 Definitions

Definition 3.1. *Covariate shift (CS) [Storkey, 2009] is the type of dataset shift in which the marginal distributions of the covariates are assumed to change, while the labelling function is assumed stationary, i.e.:*

$$\begin{aligned} P(X) &\neq Q(X) \\ P(Y|X) &= Q(Y|X) \end{aligned}$$

This type of shift is characteristic of $X \rightarrow Y$ problems [Fawcett and Flach, 2005], i.e., of causal learning where we are interested in predicting effects from causes. In problems affected by CS, it is often convenient to factorize the joint distribution as $P(X, Y) = P(Y|X)P(X)$.

Definition 3.2. *Prior probability shift [Storkey, 2009], variously called label shift [Lipton et al., 2018] (LS) or class-prior change [du Plessis and Sugiyama, 2012], is the type of dataset shift in which the class proportions are assumed to change, while the class-conditional densities of the covariates are assumed stationary, i.e.:*

$$\begin{aligned} P(Y) &\neq Q(Y) \\ P(X|Y) &= Q(X|Y) \end{aligned}$$

This type of shift is characteristic of $Y \rightarrow X$ problems [Fawcett and Flach, 2005], i.e., of anti-causal learning where we are interested in predicting causes from effects. In problems affected by LS, it is often convenient to factorize the joint distribution as $P(X, Y) = P(X|Y)P(Y)$.

Remark 1. *Given any deterministic measurable function $f : \mathcal{X} \rightarrow \mathbb{R}$, the LS assumption $P(X|Y) = Q(X|Y)$ implies $P(f(X)|Y) = Q(f(X)|Y)$ [Lipton et al., 2018, Lemma 1]. This has important implications when we take $f = \tilde{h}$ (our crisp classifier), as this implies that the class-conditional distribution of the classifier predictions is stationary, i.e., $P(\tilde{Y}|Y) = Q(\tilde{Y}|Y)$. Similarly, if we take $f = \tilde{h}$ (our probabilistic classifier) it holds that $P(\tilde{Y}|Y) = Q(\tilde{Y}|Y)$.*

Definition 3.3. *A calibrator $\zeta : \mathcal{H} \times \mathcal{S} \rightarrow \mathcal{H}$ is a model that takes as input an uncalibrated classifier $h \in \mathcal{H}$ and a reference unlabelled set $D \in \mathcal{S}$, and generates a classifier \tilde{h} which is calibrated with respect to D . A perfect calibrator ζ^* is such that the classifier $\tilde{h}^* = \zeta^*(h, D)$ it returns is perfectly calibrated with respect to D , which in turn means for all outcomes $\tilde{y} \in [0, 1]$ of \tilde{h}^* the following condition holds true:*

$$\tilde{y} = \frac{|\{x \in D : \Phi(x) = 1, \tilde{h}^*(x) = \tilde{y}\}|}{|\{x \in D : \tilde{h}^*(x) = \tilde{y}\}|} \quad (1)$$

that is, the value \tilde{y} corresponds to the true proportion of positives among all elements for which the classifier assigns the same value.

Asymptotically, i.e., that when the sample D approximates the entire population D^∞ , the calibrated classifier $\tilde{h}^ = \zeta^*(h, D^\infty)$ is such that for all $\tilde{y} = \tilde{h}^*(x)$:*

$$\tilde{y} = Q(Y = 1 | \tilde{Y} = \tilde{y}) \quad (2)$$

Remark 2. *Note that the notion of calibration is not necessarily tied to classifier accuracy [Silva Filho et al., 2023]; in other words, a perfectly calibrated classifier is not equivalent to a perfect classifier. For example, if a classifier is perfectly calibrated and returns the posterior probability $\tilde{h}^*(x) = 0.60$ for some x , this means that predicting x belongs to the positive class (e.g., by thresholding at $t = 0.5$) has 40% chance of being mistaken.*

Remark 3. *Note also that our definition of a calibrator function does not align with the more traditional one, in which the calibrator function is given access to the class labels of the datapoints in the reference set. Conversely, our notion of calibration aligns well with more recent work on calibration in the context of dataset shift (see, e.g., [Wang et al., 2020, Popordanoska et al., 2024]).*

Definition 3.4. *A binary quantifier is a model $\rho : \mathcal{S} \rightarrow [0, 1]$ that predicts the fraction of positive instances in a sample. A perfect quantifier ρ^* is such that:*

$$\rho^*(D) = \frac{|\{x \in D : \Phi(x) = 1\}|}{|D|} \quad (3)$$

With respect to the population, the perfect quantifier returns the prior of the positive class in the underlying distribution, i.e.:

$$\rho^*(D^\infty) = Q(Y = 1) \quad (4)$$

Definition 3.5. A predictor of classifier accuracy is a model $\alpha : \mathcal{H} \times \mathcal{S} \rightarrow [0, 1]$ that takes as input a classifier $h \in \mathcal{H}$ and a reference set $D \in \mathcal{S}$ and predicts the accuracy h will have on D . A perfect predictor of classifier accuracy satisfies:

$$\alpha^*(h, D) = \frac{|\{x \in D : \Phi(x) = h(x)\}|}{|D|} \quad (5)$$

At the population level, the predictor α^* returns the probability that the predictions of h are correct in the underlying distribution, i.e.:

$$\alpha^*(h, D^\infty) = Q(Y = \hat{Y}) \quad (6)$$

Remark 4. While the term accuracy is generally used to denote any evaluation measure of classifier performance, our definition is bounded to the case in which such measure is taken to be vanilla accuracy, i.e., the fraction of correctly classified instances.

4 Problem Equivalences via Reduction

In this section, we focus our attention to the binary case, and show that the three problems are equivalent via reduction. That is, we show that a perfect model for one of the problems would enable a perfect solution for the other two. In what follows, we cover the cases in which we assume access to a perfect calibrator ζ^* (Section 4.1), access to a perfect quantifier ρ^* (Section 4.2), and access to a perfect estimator of classifier accuracy α^* (Section 4.3).

4.1 Access to a Perfect Calibrator ζ^*

Let us assume we have access to a perfect calibrator and try to attain perfect models for quantification (Lemma 1) and classifier accuracy prediction (Lemma 2).

Lemma 1. $\zeta^* \implies \rho^*$, i.e., from a perfect calibrator we can attain a perfect quantifier.

Proof. Let $\tilde{h}^* = \zeta^*(h, D)$ be a perfectly calibrated classifier with respect to D . Consider the following estimator:

$$E(\tilde{h}^*, D) \stackrel{\text{def}}{=} \frac{1}{|D|} \sum_{x_i \in D} \tilde{h}^*(x_i) = \frac{1}{|D|} \sum_{x_i \in D} \tilde{y}_i \quad (7)$$

This summation can be equivalently rewritten as a sum of unique posterior values \tilde{y} in $U = \{\tilde{h}^*(x_i) : x_i \in D\}$, each multiplied by the total number of times it appears in the sequence, i.e., multiplied by $|\{x_i \in D : \tilde{h}^*(x_i) = \tilde{y}\}|$. Note that some classifiers might assign the same posterior value to several datapoints. For example, some implementations of the probabilistic k -NN classifier will at most assign $k + 1$ different such values; decision trees may assign the same posterior value to every datapoint assigned to the same leaf node of a decision tree. Other classifiers, however, might potentially assign different probabilities to every datapoint in D [Flach and Webb, 2016]. While this has implications in practical cases, it does not compromise the proof whatsoever. It thus follows that:

$$E(\tilde{h}^*, D) = \frac{1}{|D|} \sum_{\tilde{y}_j \in U} \left(\tilde{y}_j \cdot |\{x_i \in D : \tilde{h}^*(x_i) = \tilde{y}_j\}| \right)$$

Substituting \tilde{y}_j by the definition of a perfectly calibrated classifier (Equation 1) it follows that

$$\begin{aligned} E(\tilde{h}^*, D) &= \frac{1}{|D|} \left(\sum_{\tilde{y}_j \in U} \frac{|\{x_i \in D : \Phi(x_i) = 1, \tilde{h}^*(x_i) = \tilde{y}_j\}|}{|\{x_i \in D : \tilde{h}^*(x_i) = \tilde{y}_j\}|} \cdot |\{x_i \in D : \tilde{h}^*(x_i) = \tilde{y}_j\}| \right) \\ &= \frac{1}{|D|} \sum_{\tilde{y}_j \in U} |\{x_i \in D : \Phi(x_i) = 1, \tilde{h}^*(x_i) = \tilde{y}_j\}| \\ &= \frac{1}{|D|} |\{x_i \in D : \Phi(x_i) = 1\}| \\ &= \rho^*(D) \end{aligned}$$

which completes the proof. Note this estimator is also consistent at the population level; i.e., that $E(\tilde{h}^*, D^\infty) = \rho^*(D^\infty)$, since

$$E(\tilde{h}^*, D^\infty) = \mathbb{E}_{X \sim Q_X}[\tilde{h}^*(X)] = \mathbb{E}_{X \sim Q_X}[\tilde{Y}] = \int_{\mathcal{X}} \tilde{y} \cdot Q(x) \, dx \quad (8)$$

where we replace \tilde{y} with its definition in the asymptomatic case (Equation 2) and change the integration variable x in favour of \tilde{y} , that subsumes all datapoints x for which $\tilde{h}^*(x) = \tilde{y}$ (that is, where $Q(\tilde{Y} = \tilde{y}) = \int_{x : \tilde{h}^*(x) = \tilde{y}} Q(X = x) dx$) thus obtaining

$$E(\tilde{h}^*, D^\infty) = \int_0^1 Q(Y = 1 | \tilde{Y} = \tilde{y}) \cdot Q(\tilde{Y} = \tilde{y}) d\tilde{y} = Q(Y = 1) \quad (9)$$

□

Lemma 2. $\zeta^* \implies \alpha^*$, i.e., from a perfect calibrator we can attain a perfect estimator of classifier accuracy.

Proof. Consider the following partition over D :

$$\begin{aligned} D_\oplus &= \{x \in D : h(x) = 1\} \\ D_\ominus &= \{x \in D : h(x) = 0\} \end{aligned} \quad (10)$$

Let us generate two perfectly calibrated classifiers, $\tilde{h}_\oplus^* = \zeta^*(h, D_\oplus)$ and $\tilde{h}_\ominus^* = \zeta^*(h, D_\ominus)$ for each of these parts, respectively. Now, consider the following estimator of classifier accuracy:

$$E(h, D, \zeta^*) \stackrel{\text{def}}{=} \frac{\sum_{x_i \in D_\oplus} \tilde{h}_\oplus^*(x_i) + \sum_{x_j \in D_\ominus} (1 - \tilde{h}_\ominus^*(x_j))}{|D|} \quad (11)$$

We can equivalently express the summations as the sum of unique values in $U_\oplus = \{\tilde{h}_\oplus^*(x) : x \in D_\oplus\}$ and $U_\ominus = \{\tilde{h}_\ominus^*(x) : x \in D_\ominus\}$, each multiplied by the number of times each value appears in the sequence:

$$\begin{aligned} E(h, D, \zeta^*) &= \frac{\sum_{\tilde{y}_\oplus \in U_\oplus} \tilde{y}_\oplus \cdot |\{x_i \in D_\oplus : \tilde{h}_\oplus^*(x_i) = \tilde{y}_\oplus\}|}{|D|} \\ &\quad + \frac{\sum_{\tilde{y}_\ominus \in U_\ominus} (1 - \tilde{y}_\ominus) \cdot |\{x_j \in D_\ominus : \tilde{h}_\ominus^*(x_j) = \tilde{y}_\ominus\}|}{|D|} \end{aligned} \quad (12)$$

By the definition of perfect calibration it follows that

$$\begin{aligned} (1 - \tilde{y}) &= 1 - \frac{|\{x \in D : \Phi(x) = 1, \tilde{h}^*(x) = \tilde{y}\}|}{|\{x \in D : \tilde{h}^*(x) = \tilde{y}\}|} \\ &= \frac{|\{x \in D : \Phi(x) = 0, \tilde{h}^*(x) = \tilde{y}\}|}{|\{x \in D : \tilde{h}^*(x) = \tilde{y}\}|} \end{aligned} \quad (13)$$

i.e., that the computing the complement $(1 - \tilde{y})$ of a well-calibrated value \tilde{y} has the effect of “switching” from $\Phi(x) = 1$ to $\Phi(x) = 0$ in the numerator of Equation 1. Note also that, by multiplying both sides of Equation 1 by the denominator of the right-most part, we obtain:

$$\tilde{y} \cdot |\{x \in D : \tilde{h}^*(x) = \tilde{y}\}| = |\{x \in D : \Phi(x) = 1, \tilde{h}^*(x) = \tilde{y}\}|$$

if we do the same multiplication in Equation 13, we can turn back to Equation 12 and continue as follows:

$$\begin{aligned} E(h, D, \zeta^*) &= \frac{\sum_{\tilde{y}_\oplus \in U_\oplus} |\{x_i \in D_\oplus : \Phi(x_i) = 1, \tilde{h}_\oplus^*(x_i) = \tilde{y}_\oplus\}|}{|D|} \\ &\quad + \frac{\sum_{\tilde{y}_\ominus \in U_\ominus} |\{x_j \in D_\ominus : \Phi(x_j) = 0, \tilde{h}_\ominus^*(x_j) = \tilde{y}_\ominus\}|}{|D|} \\ &= \frac{|\{x_i \in D_\oplus : \Phi(x_i) = 1\}| + |\{x_j \in D_\ominus : \Phi(x_j) = 0\}|}{|D|} \\ &= \frac{|\{x \in D : \Phi(x) = h(x)\}|}{|D|} \\ &= \alpha^*(h, D) \end{aligned}$$

This estimator is consistent at the population level as well. Note that, in the asymptotic case, Equation 11 can be rewritten as two expected values:

$$E(h, D^\infty, \zeta^*) = \mathbb{E}_{X \sim Q_{X|\hat{Y}=1}}[\tilde{h}_\oplus^*(X)]Q(\hat{Y}=1) + \left(1 - \mathbb{E}_{X \sim Q_{X|\hat{Y}=0}}[\tilde{h}_\ominus^*(X)]\right)Q(\hat{Y}=0)$$

By virtue of Equations 8 and 9, we can replace the expected values with the corresponding (conditional) distributions of the priors as follows

$$\begin{aligned} E(h, D, \zeta^*) &= Q(Y=1|\hat{Y}=1)Q(\hat{Y}=1) + (1 - Q(Y=1|\hat{Y}=0))Q(\hat{Y}=0) \\ &= Q(Y=1|\hat{Y}=1)Q(\hat{Y}=1) + Q(Y=0|\hat{Y}=0)Q(\hat{Y}=0) \\ &= Q(Y=1, \hat{Y}=1) + Q(Y=0, \hat{Y}=0) \\ &= Q(Y=\hat{Y}) \end{aligned}$$

□

4.2 Access to a Perfect Quantifier ρ^*

In this case, we will assume the availability of a perfect quantifier and we will try to attain perfect models for calibration (Lemma 3) and classifier accuracy prediction (Lemma 4).

Lemma 3. $\rho^* \implies \zeta^*$, i.e., from a perfect quantifier we can attain a perfect calibrator.

Proof. Consider the following estimator $E(h, \rho^*, D) \equiv \tilde{h}$ that we implement using the quantifier oracle as:

$$\tilde{h}(x) \stackrel{\text{def}}{=} \rho^*(\{x' \in D : h(x) = h(x')\}) \quad (14)$$

To simplify the notation, we define the equivalence relation $x \sim_h x'$ which induces the equivalence class

$$[x]_h = \{x' \in D : h(x) = h(x')\}$$

that is, the set of all datapoints to which the uncalibrated classifier h assigns the same value it assigns to x . This allows us to express our estimator more compactly as:

$$\tilde{h}(x) := \rho^*([x]_h) \quad (15)$$

Similarly, we can define the equivalence relation $x \sim_{\tilde{h}} x'$ that induces the equivalence class

$$[x]_{\tilde{h}} = \{x' \in D : \tilde{h}(x) = \tilde{h}(x')\} \quad (16)$$

Using this notation, it is worth noting that if \tilde{h} is perfectly calibrated, then, by definition, it can be rewritten as $\tilde{h}(x) = \rho^*([x]_{\tilde{h}})$ (see Equation 1). The proof thus consists of verifying whether $\rho^*([x]_{\tilde{h}}) = \rho^*([x]_h)$ holds true.

Let us begin by noting that $x \sim_h x' \implies x \sim_{\tilde{h}} x'$ (i.e., that $x' \in [x]_h \implies x' \in [x]_{\tilde{h}}$), while the converse implication is not necessarily true. This implicitly means that the partition of D induced by $\sim_{\tilde{h}}$ is *coarser-grained* than the partition of D induced by \sim_h or, in other words, that an equivalence class of \tilde{h} might contain more than one equivalence classes of h . Let us define the indices that enumerate the parts of $[x]_{\tilde{h}}$ as:

$$I_x = \{i \in \mathbb{N} : [x']_h^{(i)} \subseteq [x]_{\tilde{h}}\} \quad (17)$$

Such that $[x]_{\tilde{h}} = \bigcup_{i \in I_x} [x']_h^{(i)}$ with $i \neq j \implies [x']_h^{(i)} \cap [x']_h^{(j)} = \emptyset$. In the following derivation, we leverage the fact that the prevalence of a partitioned set can be computed as the number of positives in each partition (which we can easily obtain by multiplying the prevalence of that part by its cardinality) divided by the total number of elements in the set.² In this way

$$\rho^*([x]_{\tilde{h}}) = \rho^*(\bigcup_{i \in I_x} [x']_h^{(i)}) \quad (18)$$

$$= \frac{\sum_{i \in I_x} \rho^*([x']_h^{(i)}) \cdot |[x']_h^{(i)}|}{|[x]_{\tilde{h}}|} \quad (19)$$

²That is, given a set \mathcal{A} partitioned as A_1, \dots, A_k , such that $\mathcal{A} = \bigcup_{i=1}^k A_i$ with $A_i \cap A_j = \emptyset$ for $i \neq j$, the prevalence of \mathcal{A} can be obtained as $\rho^*(\mathcal{A}) = \frac{1}{|\mathcal{A}|} \sum_{i=1}^k (\rho^*(A_i) \cdot |A_i|)$.

By the definition of $[x]_{\tilde{h}}$ (see Equations 15, 16), all its elements are such that $x', x'' \in [x]_{\tilde{h}} \implies \rho^*([x']_h) = \rho^*([x'']_h)$, that is, the class prevalence of $p_i = \rho^*([x']_h^{(i)})$ is the same for all equivalence classes that compose $[x]_{\tilde{h}}$, i.e., $p_i = p_j, \forall i, j \in I_x$. Let us simply call p this (constant) prevalence value that we factor out as follows:

$$\rho^*([x]_{\tilde{h}}) = \frac{p \cdot \sum_{i \in I_x} |[x']_h^{(i)}|}{|[x]_{\tilde{h}}|} = p \quad (20)$$

The proof for the finite sample is completed by realising that p is also the prevalence value of $[x]_h$, which is one of the elements in the partition, i.e., $p = \rho^*([x]_h)$, and therefore it follows that $p = \rho^*([x]_{\tilde{h}}) = \rho^*([x]_h)$ meaning that the classifier \tilde{h} was indeed well-calibrated.

At the population level the estimator of Equation 15 corresponds to:

$$\tilde{h}(x) \stackrel{\text{def}}{=} Q(Y = 1 | h(X) = h(x)) \quad (21)$$

If \tilde{h} were well-calibrated, then the following would also hold true

$$\tilde{h}(x) = Q(Y = 1 | \tilde{h}(X) = \tilde{h}(x)) \quad (22)$$

so we need to prove whether $Q(Y = 1 | h(X) = h(x)) = Q(Y = 1 | \tilde{h}(X) = \tilde{h}(x))$ is true. To this aim, let us begin by applying the definition of conditional probability to Equation 22:

$$\tilde{h}(x) = \frac{Q(Y = 1, \tilde{h}(X) = \tilde{h}(x))}{Q(\tilde{h}(X) = \tilde{h}(x))}$$

Since, as we saw before, the random variable $\tilde{h}(X) = \tilde{Y}$ induces a coarser-grained partition of \mathcal{X} than $h(X)$, we can “unpack” the probability density of the former as an aggregation of all the corresponding cases of the latter. Let $\tilde{y} = \tilde{h}(x)$ so we can rewrite:

$$\begin{aligned} Q(\tilde{h}(X) = \tilde{y}) &= \sum_{w \in \mathcal{W}_{\tilde{y}}} Q(h(X) = w) \\ Q(Y = 1, \tilde{h}(X) = \tilde{y}) &= \sum_{w \in \mathcal{W}_{\tilde{y}}} Q(Y = 1, h(X) = w) \end{aligned}$$

with $\mathcal{W}_{\tilde{y}} = \{h(x') : \rho^*([x']_h) = \tilde{y}\}$. Now, we can proceed from where we left off as follows:

$$\begin{aligned} \tilde{h}(x) &= \frac{\sum_{w \in \mathcal{W}_{\tilde{y}}} Q(Y = 1, h(X) = w)}{\sum_{w \in \mathcal{W}_{\tilde{y}}} Q(h(X) = w)} \\ &= \frac{\sum_{w \in \mathcal{W}_{\tilde{y}}} Q(Y = 1 | h(X) = w) Q(h(X) = w)}{\sum_{w \in \mathcal{W}_{\tilde{y}}} Q(h(X) = w)} \end{aligned}$$

and since we know, by the construction of $\mathcal{W}_{\tilde{y}}$, that the value of $Q(Y = 1 | h(X) = w)$ is the same constant value for all the choices of $w \in \mathcal{W}_{\tilde{y}}$, and since we know $h(x) \in \mathcal{W}_{\tilde{y}}$, we can factor it out from the summation as follows:

$$\begin{aligned} \tilde{h}(x) &= Q(Y = 1 | h(X) = h(x)) \cdot \frac{\sum_{w \in \mathcal{W}_{\tilde{y}}} Q(h(X) = w)}{\sum_{w \in \mathcal{W}_{\tilde{y}}} Q(h(X) = w)} \\ &= Q(Y = 1 | h(X) = h(x)) \end{aligned}$$

Which coincides with Equation 21 thus proving that \tilde{h} is indeed well-calibrated also at the population level. □

Lemma 4. $\rho^* \implies \alpha^*$, i.e., from a perfect quantifier we can attain a perfect estimator of classifier accuracy.

Proof. The proof is immediate by reusing Lemma 3 and Lemma 2:

$$\begin{aligned} \rho^* &\implies \zeta^* \quad (\text{Lemma 3}) \\ \zeta^* &\implies \alpha^* \quad (\text{Lemma 2}) \end{aligned}$$

□

4.3 Access to a Perfect Estimator of Classifier Accuracy α^*

We now assume the availability of a perfect estimator of classifier accuracy and try to attain perfect models for quantification (Lemma 5) and calibration (Lemma 6).

Lemma 5. $\alpha^* \implies \rho^*$, i.e., from a perfect estimator of classifier accuracy we can attain a perfect quantifier.

Proof. Let us reuse the partitions D_\oplus and D_\ominus produced by the classifier predictions (see Equations 10) and define the following estimator of class prevalence:

$$E(h, D, \alpha^*) \stackrel{\text{def}}{=} \alpha^*(h, D_\oplus) \frac{|D_\oplus|}{|D|} + (1 - \alpha^*(h, D_\ominus)) \frac{|D_\ominus|}{|D|} \quad (23)$$

From the definition of a perfect estimator of classifier accuracy (Equation 5), it follows that

$$\begin{aligned} E(h, D, \alpha^*) &= \frac{|\{x \in D_\oplus : h(x) = \Phi(x)\}|}{|D_\oplus|} \frac{|D_\oplus|}{|D|} + \left(1 - \frac{|\{x \in D_\ominus : h(x) = \Phi(x)\}|}{|D_\ominus|}\right) \frac{|D_\ominus|}{|D|} \\ &= \frac{|\{x \in D_\oplus : h(x) = \Phi(x)\}|}{|D|} + \frac{|D_\ominus| - |\{x \in D_\ominus : h(x) = \Phi(x)\}|}{|D|} \\ &= \frac{|\{x \in D_\oplus : h(x) = \Phi(x)\}|}{|D|} + \frac{|\{x \in D_\ominus : h(x) \neq \Phi(x)\}|}{|D|} \end{aligned}$$

and since we know $h(x) = 1$ for every $x \in D_\oplus$, and $h(x) = 0$ for every $x \in D_\ominus$, we can proceed as follows

$$\begin{aligned} E(h, D, \alpha^*) &= \frac{|\{x \in D_\oplus : h(x) = 1, \Phi(x) = 1\}| + |\{x \in D_\ominus : h(x) = 0, \Phi(x) = 1\}|}{|D|} \\ &= \frac{|\{x \in D : \Phi(x) = 1\}|}{|D|} \\ &= \rho^*(D) \end{aligned}$$

That this estimator is also consistent at the population level follows from the fact that

$$\begin{aligned} \alpha^*(h, D_\oplus^\infty) &= Q(Y = \hat{Y} | \hat{Y} = 1) \\ 1 - \alpha^*(h, D_\ominus^\infty) &= Q(Y \neq \hat{Y} | \hat{Y} = 0) \end{aligned}$$

which allows us to rewrite Equation 23 as

$$\begin{aligned} E(h, D^\infty, \alpha^*) &= Q(Y = \hat{Y} | \hat{Y} = 1) Q(\hat{Y} = 1) + Q(Y \neq \hat{Y} | \hat{Y} = 0) Q(\hat{Y} = 0) \\ &= Q(Y = \hat{Y}, \hat{Y} = 1) + Q(Y \neq \hat{Y}, \hat{Y} = 0) \\ &= Q(Y = 1, \hat{Y} = 1) + Q(Y = 1, \hat{Y} = 0) \\ &= Q(Y = 1) \end{aligned}$$

□

Lemma 6. $\alpha^* \implies \zeta^*$, i.e., from a perfect estimator of classifier accuracy we can attain a perfect calibrator.

Proof. The proof follows by transitivity using Lemma 5 and Lemma 3:

$$\begin{aligned} \alpha^* &\implies \rho^* \quad (\text{Lemma 5}) \\ \rho^* &\implies \zeta^* \quad (\text{Lemma 3}) \end{aligned}$$

□

5 Methods

In this section, we reuse the intuitions behind the proofs of Section 4 to propose direct adaptations of methods originally proposed for calibration, quantification, or classifier accuracy prediction, that allow them to be applied to the other problems. Additionally, we present two new original methods for calibration which exploit intuitions borrowed from the quantification literature in Section 5.2.

The problem setting is as follows. Let us assume to have access to a labelled D_{tr} , drawn from the training distribution P , and an unlabelled set D_{te} , drawn from the test distribution Q (see Section 3.1). We assume P and Q are related to each other by CS or LS. D_{tr} is partitioned, in a stratified way, into D_h , that we use to generate a raw (uncalibrated) probabilistic classifier h , and D_{val} , that we use to generate the corresponding estimator depending on the target task, as follows:

- In calibration experiments, h is the classifier we need to calibrate. The calibrator ζ is given access to D_{val} and the (unlabelled) set D_{te} , and is required to generate \tilde{h} , a variant of h calibrated for D_{te} .
- All quantification methods we will consider are of type *aggregative*, i.e., are methods that, in order to predict the class priors, learn a permutation-invariant function aggregating the posterior probabilities returned by a classifier. In this case, h acts as the surrogate classifier that a quantifier ρ uses to represent the datapoints in D_{val} on which the aggregation function is modelled. The same classifier is also used to represent the datapoints in D_{te} with which the aggregation function predicts the class proportions.
- When classifier accuracy prediction is the goal, h represents the classifier whose accuracy we want to estimate on D_{te} , and D_{val} is used to train a predictive model of classifier performance.

5.1 Direct Adaptations

By “direct adaptation”, we mean the process of taking one of the estimators presented in the proofs of Section 4 and replacing the oracle it depends on with an actual surrogate method. This also implies making decisions about how the surrogate model is trained, since the oracles of the proofs were assumed to be ready-to-use functions that necessitate no training. These proofs also relied on continuous random variables which sometimes need to be quantized in order to become operable.

We denote by M_{a2z} the direct adaptation of method M , originally proposed for problem a , to be used as a surrogate method for addressing problem z , with $a, z \in \{\zeta, \rho, \alpha\}$. For example, by $\text{PACC}_{\rho2\zeta}$ we denote an adaptation of the quantification method PACC to generate a calibration method.

- **The $\zeta2\rho$ method** is the simplest one. It uses a calibrator method ζ to generate, based on D_{val} (labelled) and D_{te} (unlabelled), a version \tilde{h} of h calibrated for D_{te} . The quantification task is performed by computing the average of the calibrated posteriors, as a direct application of Lemma 1 (Equation 7).
- **The $\zeta2\alpha$ method** first uses h to split D_{val} and D_{te} into $\{D_{val}^{\oplus}, D_{val}^{\ominus}\}$ and $\{D_{te}^{\oplus}, D_{te}^{\ominus}\}$, respectively (see Equation 10). Two calibrated versions \tilde{h}_{\oplus} and \tilde{h}_{\ominus} are generated using the corresponding partitions, and the final estimate of classifier accuracy is returned by applying Equation 11 of Lemma 2 on D_{te} .
- **The $\rho2\zeta$ method** first trains a quantifier ρ using the posterior probabilities of the instances in D_{val} . The method requires quantizing the posteriors of the test datapoints estimated by h . Given the hyperparameter b indicating the number of bins, we generate an isometric binning of the posteriors probabilities of the test instances, and then estimate, for the test instances falling within each bin i , the prevalence p_i of the positive class using the quantification method ρ . Such estimates might not be monotonically increasing (e.g., \hat{p}_i can happen to be higher than \hat{p}_j , with $i < j$); in such cases we enforce monotonicity by simply applying the rule $p'_i = \max\{\hat{p}_{i-1}, \hat{p}_i\}$. To reduce abrupt changes between nearby bins, we also apply average smoothing with a window size of 1; that is, we zero-pad the sequence adding $p'_0 = 0$ and $p'_{b+1} = 1$ and then apply $p''_i = \frac{1}{3}(p'_{i-1} + p'_i + p'_{i+1})$ for $1 \leq i \leq b$. Finally, and in order to avoid that at most b different calibrated posteriors are returned, we treat every value p''_i as the calibrated output for the bin center c_i , and the final calibration map is defined as a linear interpolation in the (input, output) sequence $[(0, 0), (c_1, p''_1), \dots, (c_b, p''_b), (1, 1)]$.
- **The $\rho2\alpha$ method** consists of first splitting D_{val} into $\{D_{val}^{\oplus}, D_{val}^{\ominus}\}$ using h , and then learning two dedicated quantifiers ρ^{\oplus} and ρ^{\ominus} on the corresponding partitions. At inference time, the test set D_{te} is split into $\{D_{te}^{\oplus}, D_{te}^{\ominus}\}$ using h , and we use our quantifiers to estimate the proportion of positive instances in the predicted positives ($\hat{p}^{\oplus} = \rho^{\oplus}(D_{te}^{\oplus})$) and the proportion of positive instances in the predicted negatives ($\hat{p}^{\ominus} = \rho^{\ominus}(D_{te}^{\ominus})$); the final estimate of classifier accuracy is computed as

$$\text{acc} = \frac{\hat{p}^{\oplus} \cdot |D_{te}^{\oplus}| + (1 - \hat{p}^{\ominus}) \cdot |D_{te}^{\ominus}|}{|D_{te}|}$$

- **The $\alpha2\rho$ method** partitions D_{val} into $\{D_{val}^{\oplus}, D_{val}^{\ominus}\}$ using h , and then learns two dedicated estimators of classifier accuracy, α^{\oplus} and α^{\ominus} , on the corresponding partitions. At inference time, the test set D_{te} is split into $\{D_{te}^{\oplus}, D_{te}^{\ominus}\}$ using h , and two estimates of classifier accuracy are computed on the corresponding sets as

$\hat{\text{acc}}^\oplus = \alpha^\oplus(h, D_{te}^\oplus)$ and $\hat{\text{acc}}^\ominus = \alpha^\ominus(h, D_{te}^\ominus)$. The final prevalence is computed by plug-in these estimates into Equation 23 of Lemma 5.

- **The $\alpha 2\zeta$ method** is similar to the $\rho 2\zeta$ approach; it trains a classifier accuracy prediction method α on D_{val} and quantizes the posteriors of the instances in D_{te} produced by h using isometric binning for b bins. A sequence (a_1, \dots, a_b) of accuracy estimates for the b bins is generated using α . In this case, b needs to be even, so that a_i accounts for the fraction of positive instances in bins above 0.5 (i.e., when $\frac{b}{2} < i \leq b$), while the fraction of positive instances for bins below 0.5 (i.e., when $1 \leq i \leq \frac{b}{2}$) is instead estimated as $(1 - a_i)$. This way, a sequence of (input, output) values $[(0, 0), (c_1, 1 - a_1), \dots, (c_{\frac{b}{2}}, 1 - a_{\frac{b}{2}}), (c_{\frac{b}{2}+1}, a_{\frac{b}{2}+1}), \dots, (c_b, a_b), (1, 1)]$ for the calibration map is generated. We impose monotonicity and smooth the sequence, which is finally used to define a calibration map via interpolation as before.

5.2 Original New Methods for Calibration

In this section, we propose two new calibration methods that gain inspiration from quantification methods.

5.2.1 PacCal: a new calibration method based on PACC

The first of the new calibration methods we propose gains inspiration from the “probabilistic adjusted classify and count” (PACC) quantification method [Bella et al., 2010] and is designed to calibrate a classifier under LS. Let us denote by \tilde{h} (instead of by h) our classifier, to emphasize the fact that it needs to be a probabilistic classifier (we do not make any assumption about whether it has been calibrated on the training distribution or not, though). Let us briefly recap the rationale behind PACC, which rests on the following observation:

$$\begin{aligned} Q(\tilde{Y} = 1) &= Q(\tilde{Y} = 1|Y = 1) \cdot Q(Y = 1) + Q(\tilde{Y} = 1|Y = 0) \cdot Q(Y = 0) \\ &= P(\tilde{Y} = 1|Y = 1) \cdot Q(Y = 1) + P(\tilde{Y} = 1|Y = 0) \cdot (1 - Q(Y = 1)) \end{aligned}$$

where the replacement of the test class-conditional distributions of classifier predictions (Q) with the training ones (P) follows from Remark 1 (Section 3.2). It then follows that:

$$Q(Y = 1) = \frac{Q(\tilde{Y} = 1) - P(\tilde{Y} = 1|Y = 0)}{P(\tilde{Y} = 1|Y = 1) - P(\tilde{Y} = 1|Y = 0)}$$

The class prevalence estimate of PACC is attained by estimating $Q(\tilde{Y} = 1)$ as the average of the posterior probabilities returned by \tilde{h} on the test instances (i.e., the expected value on the empirical test sample), and replacing the class-conditional distributions with estimates of the true positive rate (tpr) and false positive rate (fpr) of the classifier obtained on held-out validation data (D_{val}), i.e.:

$$\hat{p}^{\text{PACC}} = \frac{\mathbb{E}_{x \sim D_{te}}[\tilde{h}(x)] - \hat{\text{fpr}}}{\hat{\text{tpr}} - \hat{\text{fpr}}} \quad (24)$$

Now, note that the adjustment implemented in Equation 24 is linear; we can therefore equivalently rewrite it as an affine transformation with scaling factor $\beta = \frac{1}{\hat{\text{tpr}} - \hat{\text{fpr}}}$ and intercept $\gamma = -\frac{\hat{\text{fpr}}}{\hat{\text{tpr}} - \hat{\text{fpr}}}$ as follows:

$$\hat{p}^{\text{PACC}} = \mathbb{E}_{x \sim D_{te}}[h(x)] \cdot \beta + \gamma = \mathbb{E}_{x \sim D_{te}}[h(x) \cdot \beta + \gamma] \quad (25)$$

This suggests that we can update the posterior probability of each of the test datapoints to account for the new prior using a linear transformation. This procedure thus yields a calibrated classifier:

$$\tilde{h}'(x) \stackrel{\text{def}}{=} \tilde{h}(x) \cdot \beta + \gamma \quad (26)$$

However, the linear transformation is not guaranteed to lie in the $[0, 1]$ interval. This is inherited from the well-known instability³ of PACC when the denominator of Equation 24 is small. When this happens, we simply apply a sigmoid function (σ) after the linear transformation. We thus dub PacCal ^{σ} (short for Probabilistic Adjusted Classify and Count for Calibration). The extent to which this method provides well-calibrated posteriors, in the sense of a calibration-oriented loss, is later discussed in the experimental section.

³Some methods from the quantification literature have been proposed to better handle these instabilities, including the T50, MAX, X, Median Sweep (MS), and its variant MS2; see [Forman, 2008].

5.2.2 DMcal: a new calibration method based on HDy

The second original calibration method we propose is also based on a quantification method designed to work under LS conditions: the so-called Hellinger-Distance-y (HDy) method of [González-Castro et al., 2013].

HDy is a distribution-matching quantification method which relies on histograms of the posterior probabilities returned by our classifier for representing the class-conditional densities of the positive (histogram H_{val}^{\oplus}) and negative (histogram H_{val}^{\ominus}) examples in the validation set D_{val} . At inference time, the histogram H_{te} of the posterior probabilities of the test datapoints is generated, and the mixture parameter p that yields the closest match between the “validation mixture” (H_{val}^{\oplus} and H_{val}^{\ominus}) and the test distribution (H_{te}), in terms of the Hellinger Distance (HD), is returned as the class prior estimate, i.e.:

$$\hat{p}^{HDy} = \arg \min_{p \in [0,1]} \text{HD}((pH_{val}^{\oplus} + (1-p)H_{val}^{\ominus}), H_{te}) \quad (27)$$

Given two histograms of densities $H^A = (H_1^A, \dots, H_b^A)$ and $H^B = (H_1^B, \dots, H_b^B)$ of b bins, the Hellinger Distance is defined as:

$$\text{HD}(H^A, H^B) = \sqrt{1 - \sum_{i=1}^b \sqrt{H_i^A \cdot H_i^B}}$$

Once the test prevalence of the positive instances has been estimated, we can interpret the proportion of positives within each bin of the mixture as a calibrated value for that bin. More formally, the calibrated output v_i for the i -th

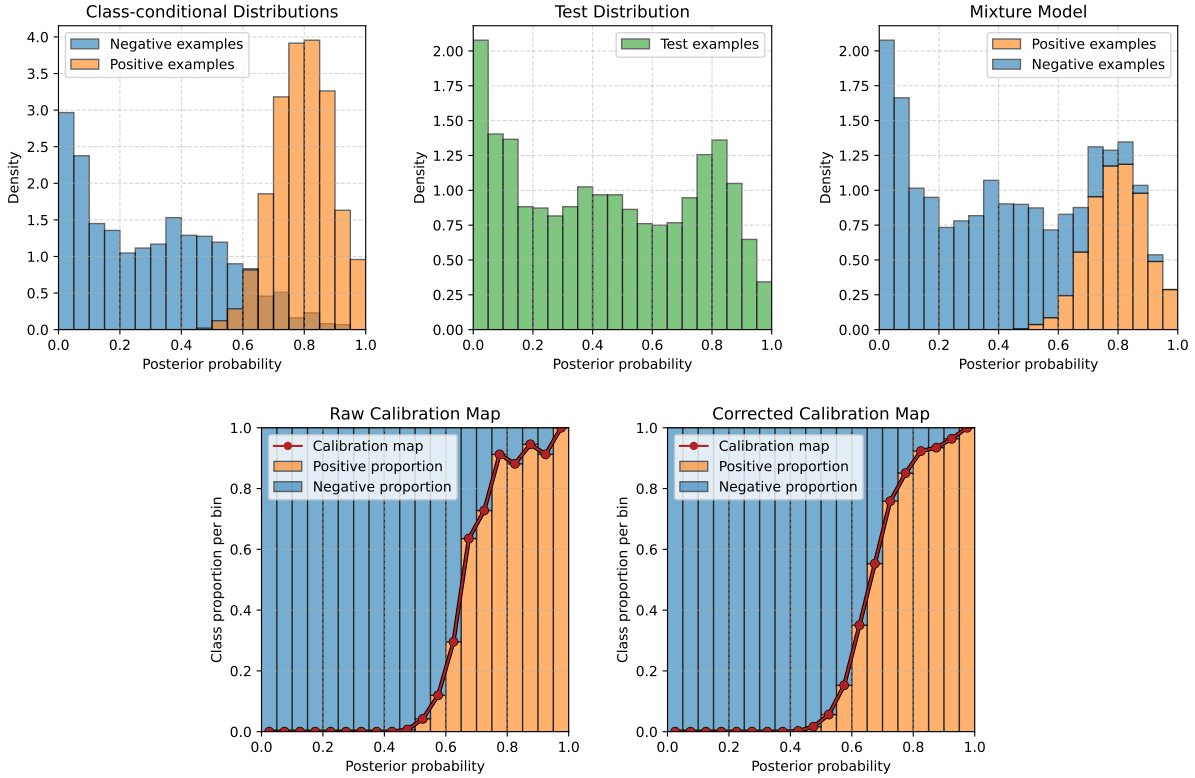


Figure 1: Graphical explanation of DMcal. First row: The left-most panel shows the class-conditional distributions, represented as histograms of posterior probabilities (H_{val}^{\ominus} in blue, and H_{val}^{\oplus} in orange) modelled on validation data. The central panel displays the test histogram (H_{te}). The right-most panel displays the mixture model of H_{val}^{\ominus} and H_{val}^{\oplus} obtained with the mixture parameter $p = 0.3$ which yields the closest mixture to the test histogram in terms of HD. Second row: the left-most panel shows a “raw” calibration map computed on the proportion of positive and negative contributions of each bin of the mixture model; the right-most panel shows the corrected calibration map after imposing monotonicity and smoothing the raw calibration map.

bin is given by:

$$v_i = \frac{\hat{p}^{\text{HDy}} \cdot H_{val,i}^{\oplus}}{\hat{p}^{\text{HDy}} \cdot H_{val,i}^{\oplus} + (1 - \hat{p}^{\text{HDy}}) \cdot H_{val,i}^{\ominus}} \quad (28)$$

To enable continuous calibration outputs and avoid returning at most b distinct output values, the calibration map is defined as a piecewise linear interpolation over the sequence of points $[(0, 0), (c_1, v_1), \dots, (c_b, v_b), (1, 1)]$, where c_i denotes the center of the i -th bin and v_i the associated calibrated value obtained with Equation 28. Finally, to avoid artifacts due to random sampling (i.e., jagged outputs), the sequence of calibrated values is post-processed to ensure monotonicity and then smoothed before defining the final calibration map. We call this method DMcal, for Distribution-Matching based Calibration; the whole process behind DMcal is illustrated in Figure 1.

Note that this method is non-parametric, i.e., it makes no assumption about the underlying distributions (other than assuming that the underlying distributions are related to each other through LS). DMcal is close in spirit to empirical binning [Zadrozny and Elkan, 2001a], with the key difference that the proportion of positives in each bin is taken from a mixture model re-parameterized with an estimated prior, and that the calibration map is post-processed to allow for continuous, monotonically increasing, and smooth outputs.

6 Experiments

This section presents our experimental evaluation of the newly proposed methods from Section 5. These methods, inspired by approaches developed for other tasks, are assessed in terms of their ability to compete with techniques natively designed for the target problem. The section is structured into three parts: calibration (Section 6.4.1), quantification (Section 6.4.2), and classifier accuracy prediction (Section 6.4.3).

Before discussing the results we have obtained, we first describe the reference methods we choose (Section 6.1), and how we simulate CS (Section 6.2) and LS (Section 6.3) in our experiments.

6.1 Reference Methods

The methodology we follow in our experiments consists of confronting three representative reference methods from each problem area against adaptations of reference methods originally proposed for the other two problems. In addition to these 9 reference methods (3 problems \times 3 methods), we also consider, in some cases, additional reference methods that enrich the comparison under specific types of dataset shift, as well as a baseline method representative of a standard IID-based solution for each problem. The reference methods selected from each problem are listed below.

- As our reference methods from calibration, we select CPCS [Park et al., 2020] and TransCal [Wang et al., 2020], which are specialized for CS, and LasCal [Popordanoska et al., 2024], which is specialized for LS. As an additional reference method for the calibration experiments, we also consider the Head2Tail [Chen and Su, 2023] calibrator which was originally described as a method for CS, but that, for reasons discussed in Section 2.1, we believe is more suited for LS. For all these methods, we relied on the implementations made available by the authors of LasCal.⁴ As our IID baseline for calibration experiments, we consider Platt scaling [Platt, 2000] and relied on the implementation of `scikit-learn`.
- The three reference methods we choose for quantification are PACC [Bella et al., 2010], EMQ [Saerens et al., 2002], and KDEy [Moreo et al., 2025], three well-established methods for LS (Section 2.2). In some cases, we also consider PCC [Bella et al., 2010] as an additional reference method for CS, and calibrated variants of EMQ [Alexandari et al., 2020]. The IID solution for quantification experiments is the naive “classify and count” (CC) approach [Forman, 2005]. In all cases, we rely on the implementations provided by the QuaPy library⁵ for quantification [Moreo et al., 2021], and leave all hyperparameters set at their default values.
- For classifier accuracy prediction, we consider ATC [Garg et al., 2022], DoC [Guillory et al., 2021], and LEAP [Volpi et al., 2024] as our reference methods (Section 2.3). The former two methods can deal with both covariate and LS, while the latter is instead bounded to LS. DoC requires a protocol for generating validation samples out of D_{val} . To this aim, we generate 100 samples $D_{val}^1, \dots, D_{val}^{100}$ of $|D_{val}^i| = 250$ instances

⁴<https://github.com/tpopordanoska/label-shift-calibration>. This repository builds on top of previous implementations including the `abstention` package for calibration <https://github.com/kundajelab/abstention>, Jiahao Chen’s calibration package for Head2Tail <https://github.com/JiahaoChen1/Calibration>, or the TransCal package <https://github.com/thuml/TransCal>, among others.

⁵<https://github.com/HLT-ISTI/QuaPy>

each using the APP protocol in experiments addressing LS (this protocol is later described in Section 6.3.1). Since the entire validation set comes from the training distribution we are not allowed to mimic the CS sampling generation protocol (which necessitates from labelled examples of the test distribution –Section 6.2.1); in this case, we simply draw 100 random samples, of 250 instances each, out of D_{val} . As our IID baseline, we consider a method that estimates the classifier’s accuracy on the held-out validation data D_{val} . We dub this method “Naive” because D_{val} comes from the training distribution, and so the method is agnostic to the presence of dataset shift. We have adapted the implementations of these methods available in the repository of LEAP.⁶

The new methods PacCal^σ and DMCAL rely on the implementations of PACC and HDy, respectively, which are available in QuaPy. For DMCAL, we set the number of bins to 8, which is the default value for the underlying quantifier HDy in QuaPy.

The code that reproduces all the experiments, and implements the adaptation methods as well as the new methods PacCal^σ and DMCAL, is available online at <https://github.com/AlexMoreo/UnifyingProblems>.

6.2 Experiments Simulating Covariate Shift

6.2.1 Sample Generation Protocol

The protocol we use to simulate CS on real data consists of selecting two classification datasets, A and B , each annotated with binary labels that are comparable across datasets. Each dataset is split into a training set (D_{tr}^A, D_{tr}^B) and a test set (D_{te}^A, D_{te}^B). The training set of A is further divided into a classifier training set (D_h^A) and a validation set (D_{val}^A). A classifier h is then generated on D_h^A from dataset A , which plays the role of the source domain. We then construct a sequence of 100 test sets $D_{te}^1, \dots, D_{te}^{100}$ of $|D_{te}^i| = 250$ instances each, as a progressively interpolated mixture of the two test sets D_{te}^A and D_{te}^B . Specifically, for each $i \in \{1, \dots, 100\}$, the test set D_{te}^i consists of $n_A^{(i)} = \lceil 250 \cdot (1 - \frac{i-1}{99}) \rceil$ instances randomly drawn from D_{te}^A , and $n_B^{(i)} = 250 - n_A^{(i)}$ instances randomly drawn from D_{te}^B . Note that every test set D_{te}^i is constructed from scratch, and not as a modification of the previous one D_{te}^{i-1} , i.e., the instances drawn from A and B in any two test sets are independent of each other and result from separate random draws. Since A and B originate from different, yet related, domains, this protocol effectively simulates varying levels of CS. The first set D_{te}^1 , composed entirely of instances from the source domain A , conforms to the IID assumption (i.e., there is no shift), whereas the last set D_{te}^{100} , composed entirely of instances from the target domain B , represents the highest level of CS. For each test set D_{te}^i , the model under evaluation (i.e., for calibration, quantification, or classifier accuracy prediction) is given access to the classifier (h) and the validation set (D_{val}^A) from the source domain A .

We keep sample consistency across all experiments, in order to guarantee all methods are tested on the exact same training, validation, and test sets.

6.2.2 Datasets

As our datasets for CS experiments we choose three datasets of reviews for sentiment classification: IMDb⁷ (imdb) [Maas et al., 2011], Rotten Tomatoes⁸ (rt) [Pang and Lee, 2005], and Yelp Reviews⁹ (yelp) [Zhang et al., 2015]. IMDb and Rotten Tomatoes already come with binary labels. For the Yelp Reviews we convert the 5-star ratings into binary labels by removing all instances labelled with 3 stars, and then treating 1 and 2 stars as negative reviews and 4 and 5 stars as positive reviews. The three datasets are related, as they all contain opinion data, yet they differ in various aspects. Although IMDb and Rotten Tomatoes both consists of movie reviews, the reviews in IMDb are generated by registered users and are typically longer than those from Rotten Tomatoes, which are instead short reviews generated by professional critics. The Yelp Reviews is more different, as its reviews are not about movies, but rather about different businesses. All datasets are perfectly balanced; some statistics of the datasets we use (after filtering) are summarized in Table 1.

When we apply the sample generation protocol discussed above, the three datasets take turns in a “round robin” fashion, acting as either the source or the target domain. For example, “yelp→rt” denotes an experiment where the Yelp Reviews is used as the source domain and test samples are generated by mixing documents from the target

⁶<https://github.com/lorenzovolpi/LEAP> This repository also reuses the original code for the method ATC available at https://github.com/saurabhgarg1996/ATC_code/

⁷Data available at <https://huggingface.co/datasets/stanfordnlp/imdb>

⁸Data available at https://huggingface.co/datasets/cornell-movie-review-data/rotten_tomatoes

⁹Data available at https://huggingface.co/datasets/Yelp/yelp_review_full

Table 1: Statistics of the sentiment datasets used in our CS experiments

Dataset	#Training	#Validation	#Test
IMDb (imdb)	25K	—	25K
Rotten Tomatoes (rt)	8.53K	1.07K	1.07K
Yelp Reviews (yelp)	520K	—	40K

domain Rotten Tomatoes. Since we are interested in simulating CS, we exclude combinations in which the same dataset plays both the role of source and target domain; we thus end up considering a total of six different source-target combinations.

6.2.3 Classifiers

As our classifiers, we consider three well-known pre-trained language models available at Huggingface¹⁰: google-bert/bert-base-uncased (hereafter BERT) [Devlin et al., 2019], distilbert/distilbert-base-uncased (hereafter DistilBERT) [Sanh et al., 2019], and FacebookAI/roberta-base (hereafter RoBERTa) [Liu et al., 2019].

In all cases, we fine-tune the classification head of each pre-trained model on the available training data for 5 epochs, using a learning rate of 5E-4 and a batch size of 64 documents. In order to prevent overfitting, we apply early stop after 5 consecutive evaluation steps (we trigger an evaluation round every 500 training steps) showing no improvement in terms of classification F_1 in validation data. When the validation set is not available (e.g., in IMDb and Yelp Reviews), we extract a held-out sample of 5,000 documents from the training set with stratification.

6.3 Experiments Simulating Label Shift

6.3.1 Sample Generation Protocol

To simulate LS, we adopt the so-called artificial-prevalence protocol (APP), a standard protocol commonly used in quantification evaluation (see [Esuli et al., 2022] for further details). Given a test set D_{te} , we generate a series of test samples $D_{te}^1, \dots, D_{te}^{100}$ each consisting of $|D_{te}^i| = 250$ instances. For each sample D_{te}^i , the APP protocol first draws a target prevalence value $p^{(i)}$, uniformly at random from the interval $[0, 1]$, which represents the desired prevalence of the positive class. Then, it draws $n_{\oplus}^{(i)} = \lceil p^{(i)} \cdot 250 \rceil$ positive and $n_{\ominus}^{(i)} = 250 - n_{\oplus}^{(i)}$ negative instances, uniformly at random from D_{te} . Regardless of the original training prevalence, this protocol ensures the generation of test samples with varying levels of LS, ranging from low shift (when $p^{(i)}$ is close to the training prevalence), to high shift (this happens when the training prevalence is close to 0 or 1 and the test prevalence $p^{(i)}$ is chosen to be close to 1 or 0, respectively).

We keep sample consistency across all experiments, in order to guarantee all methods are tested on the exact same training, validation, and test sets.

6.3.2 Datasets

For the LS experiments, we consider the 10 largest binary classification datasets from the UCI Machine Learning repository¹¹ that have been used in past quantification research (e.g., [Pérez-Gállego et al., 2017, Moreo et al., 2021]). The final selection consists of datasets cmc.3, yeast, semeion, wine-q-red, ctg.1, ctg.2, ctg.3, spambase, wine-q-white, and pageblocks.5. The dataset size ranges from a minimum of 1,473 (cmc.3) to a maximum of 5,473 (pageblocks.5). The datasets consist of tabular data, and the number of features ranges from a minimum of 8 (yeast) to a maximum of 256 (semeion). The selection includes imbalanced datasets (e.g., pageblocks.5 contains only 2.1% of positive instances, and ctg.1 contains no less than 77.8% of positives) and almost perfectly balanced ones (e.g., wine-q-red). We fetch these datasets using the QuaPy package, which also applies a standardization to the feature columns. Further details about the datasets can be consulted online.¹²

¹⁰<https://huggingface.co/>

¹¹Data available at <https://archive.ics.uci.edu>

¹²<https://hlt-isti.github.io/QuaPy/manuals/datasets.html#binary-datasets>

These datasets do not come with predefined data partitions. For each dataset, we thus generate a test partition D_{te} consisting of 30% of the whole data with stratification; the rest of the dataset is randomly split into a training set D_{tr} and a validation set D_{val} of equal size. All splits are generated with stratification.

6.3.3 Classifiers

As our classifiers for the tabular data we consider the following classifiers:

- **Logistic Regression:** is an example of a probabilistic classifier generating reasonably well-calibrated posterior probabilities (not in vain, the logistic function is used for calibration purposes [Platt, 2000]), and has almost become a standard choice for the surrogate classifier in quantification experiments (see, e.g., [Schumacher et al., 2025, Moreo et al., 2021]).
- **Naïve Bayes:** despite being a probabilistic classifier, is a typical example of an ill-calibrated classifier [Domingos and Pazzani, 1996, Zadrozny and Elkan, 2001b]. This classifier is interesting because it is widely used, partly due to its good efficiency.
- **k Nearest Neighbor:** is a representative example of instance-based learning. We set uniform weights, so that this method becomes representative of a probabilistic classifier with a fixed, limited number of possible outcomes. We set $k = 10$ so that no more than $k + 1 = 11$ different posterior probabilities (i.e., $\{0, \frac{1}{10}, \dots, \frac{9}{10}, 1\}$, the possible fractions of positive instances in the neighbourhood) can be returned.
- **Multi-Layer Perceptron:** is representative of neural approaches, which are known to be very effective in terms of classification accuracy, but that tend to provide overconfident judgments [Guo et al., 2017].

In all cases, we rely on the implementations of `scikit-learn` [Pedregosa et al., 2011] with any other hyperparameter left to its default value.

6.4 Results and Discussion

In this section, we discuss the results we have obtained for calibration (Section 6.4.1), quantification (Section 6.4.2), and classifier accuracy prediction (Section 6.4.3) experiments.

Each experiment is subdivided into two experiments, one addressing CS, and another addressing LS. We display the numerical results in tabular form, using the following notational conventions: We use a color-coding to facilitate the interpretation of results, with intense green indicating the best result for each row, and intense red indicating the worst one; the rest of the values are linearly interpolated between these two. We highlight in bold the best result for each dataset as well as all the results which are not found to be statistically significantly different from it according to a Wilcoxon signed-rank test at 95% confidence level.

We also report, in the bottom of the tables, the *win rates* (Wins) of each method with respect to the reference ones; we use $\Pr(M \succ iR)$ to indicate the percentage of all test samples (i.e., across all datasets and classifiers) in which the corresponding method has beaten at least i reference methods simultaneously, for $i \in \{1, \dots, r\}$ with r the total number of reference methods. For example, $\Pr(M \succ 2R) = 50\%$ indicates the method M has beaten two (or more) reference methods (not necessarily the same two methods every time) in half of the cases. When such value is accompanied with a \dagger symbol, it means that the win rate is statistically significant, according to a binomial test at 5% confidence level. This test considers the null hypothesis H_0 that the results of method M and those from the reference methods are indistinguishable, in which case the win rate should account for the fraction of times M happens to rank better than i reference methods in a random permutation. The null hypothesis is rejected when the total number of times (s) in which M has beaten at least i reference methods across a total of N experiments surpasses the expected probability that this would happen simply due to chance (i.e., $1 - \frac{i}{r+1}$) with r the number of reference methods), at 95% confidence level. For example, when $r = 4$ reference methods, we would expect that any method M beats exactly 3 reference methods when it ranks either first or second, and this happens in a random permutation $2/5$ of the times. More formally, this test checks whether $1 - \text{BinomialCDF}(s - 1, N, 1 - \frac{i}{r+1}) < 0.05$.

We also highlight in bold the r best average ranks in the entire table. The rationale behind this is that, should our reference methods outperform all newly proposed candidates (as one might expect), then all bolded values would be attributed to the reference methods, and none to the new candidates. Cases in which this does not happen are therefore worth analyzing.

We also analyse, in graphical form, the error as a function of the *intensity of shift*. In CS experiments, in which the test samples are generated as a mixture of source and target datasets (see Section 6.2.1), we define this intensity as the fraction of examples drawn from the target dataset, so that the intensity ranges from 0 (meaning IID conditions) to 1

(all the examples in the test set come from a different domain). In LS experiments, we measure the intensity of shift as the absolute difference between the positive prevalence in the test sample and in the training set. The intensity thus ranges from 0 (IID conditions) to values close to 1 (cases in which the proportion of positives in the training set is close to 0 but in the test is close to 1, or viceversa); note that this condition is only attainable in extreme situations, e.g., for a perfectly balance training set, the maximum achievable shift intensity is 0.5. This has the effect of generating less experiments in the high-level shift regime. This is in contrast to the level of shift generated for CS experiments, which is uniform in the interval $[0,1]$. In order to render this fact evident, we display, as a background bar-chart, the density of the number of experiments that concur at each level of shift.

Finally, for each experiment, we submit all the methods to a multiple comparison test. For this purpose, we rely on Critical Difference diagrams (CD-diagrams)¹³ [Demšar, 2006]. Following [Benavoli et al., 2016], we adopt the Wilcoxon signed-rank test for the post-hoc assessment of pairwise differences. We also apply a Holm correction and set the significance level to 0.05. Since the protocols generate test sets that are consistently aligned across all experiments, and since each one is affected by a different intensity of (prior or covariate) shift, we decided to submit all scores to the statistical test, instead of averaging them by dataset, in order to preserve the variability introduced by the sampling generation protocols and allow for a more robust comparison in this respect.

6.4.1 Calibration Experiments

The evaluation metric we use for assessing the calibration performance is the L2 Expected Calibration Error (ECE) [Popordanoska et al., 2024], given by:

$$\text{ECE} = \sum_{i=1}^b \frac{|B_i|}{n} (\text{frac}_{\text{pos}}(B_i) - \text{conf}(B_i))^2 \quad (29)$$

$$\text{frac}_{\text{pos}}(B_i) = \frac{1}{|B_i|} \sum_{j \in B_i} \mathbb{1}[y_j = 1] \quad (30)$$

$$\text{conf}(B_i) = \frac{1}{|B_i|} \sum_{j \in B_i} \tilde{h}(x_j) \quad (31)$$

where b is the number of bins, B_i is a set containing the indexes of the instances assigned to the i th bin, and $\mathbb{1}$ is the indicator function. In our experiments, we set $b = 15$ following [Popordanoska et al., 2024], but adopt isometric binning (instead of adaptative binning), in order to guarantee that all methods are evaluated with the exact same bin divisions.¹⁴ We report $100 \times \text{ECE}$ in our experiments.

We confront our reference calibration methods (Head2Tail, CPCS, TransCal, and LasCal) against our reference quantification systems (PACC, EMQ, KDEy) properly converted into calibration methods through the adaptation $\rho 2\zeta$ using 5 bins. In CS experiments, we also apply $\rho 2\zeta$ to the PCC quantification method, which is known to fare better under this type of shift [Tasche, 2022, González et al., 2024]. Analogously, we apply the $\alpha 2\zeta$ method to generate direct adaptations of our reference classifier accuracy predictors (ATC, DoC, LEAP) setting the number of bins to 6.¹⁵ In CS experiments, we propose $\text{LEAP}_{\alpha 2\zeta}^{\text{PCC}-6\text{B}}$, a variant of LEAP that replaces the original prior-shift-oriented quantifier (KDEy) with PCC, which is expected to be more reliable under CS. We also consider EMQ [Saerens et al., 2002] and the variant EMQ^{BCTS} [Alexandari et al., 2020] that previously applies an additional calibration round based on Bias-Corrected Temperature Scaling (BCTS). Based on the same principle, we explore two new configurations: $\text{EMQ}^{\text{TransCal}}$ in CS experiments and $\text{EMQ}^{\text{LasCal}}$ in LS experiments, i.e., two new methods that, in place of BCTS, apply a calibrator specialized for CS (TransCal) or LS (LasCal), respectively. Finally, we also test PacCal^σ and DMCal , the two new calibration methods proposed in Section 5.2.

The results we have obtained for CS are reported in Table 2. Somehow surprisingly, the reference methods are not excelling in this evaluation, nor even CPCS or TransCal, which were proposed for addressing CS. Among the four reference methods, the best one in terms of average ranking is TransCal, although Head2Tail obtains a higher number of best results (or results that are not statistically significantly different from the best one), which happens in 7 out of 18 cases. None of the reference methods surpass the result of the IID baseline Platt scaling, though.

¹³We use the software <https://mirkobunse.github.io/CriticalDifferenceDiagrams.jl/stable/>

¹⁴We have taken care to ensure that none of the binning-based methods use $b = 15$, in order to prevent any unintended information leak that could illegitimately favour any method in terms of ECE.

¹⁵We use 5 bins (an odd number) for $\rho 2\zeta$ and 6 bins (an even number) for $\alpha 2\zeta$ to illustrate the fact that the former works with any number of bins, while the latter requires an even number. We did not perform model selection to optimize this hyperparameter.

Table 2: Calibration performance under CS in terms of ECE

		Baselines		Reference				Adapted Methods												
		Platt	Head2Tail	CPCS	TransCal	LasCut	$PCC_{\rho 2\zeta}^{5B}$	$PACC_{\rho 2\zeta}^{5B}$	$EMQ_{\rho 2\zeta}^{5B}$	$KDE_{\rho 2\zeta}^{5B}$	$ATC_{\rho 2\zeta}^{5B}$	$DoC_{\rho 2\zeta}^{6B}$	$LEAP_{\rho 2\zeta}^{5B}$	$LEAP_{\rho 2\zeta}^{PCC-5B}$	EMQ	EMQ^{BCTS}	$EMQ^{TransCal}$	$PacCut^{\sigma}$	DMCut	
BERT	imdb→rt	0.826	2.450	2.966	1.623	0.893	0.873	1.013	1.682	2.066	0.842	0.584	1.006	0.626	3.863	2.507	14.849	0.924	2.251	
	imdb→yelp	0.587	3.026	2.314	2.051	0.743	1.047	0.699	1.038	0.875	0.634	0.611	1.191	0.886	1.867	3.141	5.325	0.638	0.630	
	rt→imdb	0.586	3.936	3.345	2.206	0.724	1.316	0.590	1.561	1.122	0.622	0.755	0.744	0.647	25.951	16.198	25.951	1.980	5.241	
	rt→yelp	0.636	3.606	3.336	2.214	0.764	1.224	0.693	0.981	1.742	0.574	0.813	0.747	0.950	25.156	2.948	25.156	2.080	1.716	
	yelp→imdb	1.467	0.782	2.632	0.876	2.642	0.767	1.179	2.125	2.592	1.445	0.964	2.357	1.689	2.742	2.581	6.785	1.430	2.393	
	yelp→rt	1.787	0.861	2.954	1.114	3.992	0.911	1.414	2.331	2.852	1.833	1.163	2.788	1.839	2.472	2.554	5.315	1.345	2.381	
DistilBERT	imdb→rt	1.076	0.729	1.560	0.922	1.923	0.700	1.140	1.836	1.854	2.643	0.827	2.138	0.936	0.954	0.873	1.088	1.052	0.904	
	imdb→yelp	0.680	0.830	1.128	0.901	1.143	0.618	0.660	1.000	0.981	1.352	0.546	1.180	0.586	0.550	0.517	1.467	1.661	0.539	
	rt→imdb	0.657	2.756	1.520	1.073	0.785	0.670	1.019	1.528	1.242	1.344	0.637	1.463	0.801	22.108	0.624	25.951	0.812	0.626	
	rt→yelp	0.830	2.131	1.811	0.905	1.131	0.580	1.370	1.998	1.422	1.455	0.651	1.981	1.246	21.334	1.395	25.155	0.767	1.184	
	yelp→imdb	1.366	0.652	1.344	0.814	2.742	0.691	0.889	1.713	1.461	1.430	0.741	1.966	1.455	1.795	1.398	3.078	2.058	1.387	
	yelp→rt	1.922	0.854	1.657	0.839	3.952	0.944	1.387	2.312	2.118	2.277	0.992	2.739	1.799	1.682	1.517	1.790	1.720	1.512	
RoBERTa	imdb→rt	1.462	0.753	2.440	0.996	2.781	0.864	1.593	2.724	2.721	4.027	1.034	2.573	0.836	3.169	3.087	6.875	0.940	2.731	
	imdb→yelp	0.637	0.777	1.676	1.115	0.841	0.738	0.637	0.926	0.909	1.089	0.622	1.031	0.583	0.600	0.596	2.045	1.509	0.589	
	rt→imdb	0.754	0.743	1.429	1.118	1.613	0.686	1.469	2.449	1.315	1.135	0.743	2.398	1.937	25.696	4.139	25.951	1.318	2.504	
	rt→yelp	0.708	0.822	1.119	1.453	1.123	0.756	1.216	1.777	1.214	1.068	0.657	2.129	1.608	24.870	3.924	25.156	1.125	2.425	
	yelp→imdb	1.047	0.610	0.731	0.551	1.547	0.615	0.578	0.899	1.067	0.889	0.668	1.210	0.792	0.598	0.881	1.163	3.585	0.852	
	yelp→rt	1.386	0.814	1.168	0.764	3.190	0.723	0.835	1.537	1.348	2.074	0.940	1.812	0.860	0.723	0.890	1.193	3.076	0.979	
Wins	Pr(M > 1R)	†94.11%	—	—	—	—	—	†97.17%	†92.50%	81.50%	†83.56%	†82.94%	†98.61%	†77.39%	†90.56%	58.28%	79.22%	38.67%	76.22%	†86.50%
	Pr(M > 2R)	†71.44%	—	—	—	—	—	†86.94%	†71.39%	46.56%	48.67%	53.11%	†89.67%	40.94%	†69.06%	43.11%	60.06%	22.94%	51.94%	†64.78%
	Pr(M > 3R)	†45.78%	—	—	—	—	—	†60.67%	†43.89%	23.94%	25.28%	31.11%	†62.44%	22.89%	†44.94%	28.33%	38.56%	12.33%	30.72%	40.61%
	Pr(M > 4R)	†25.28%	—	—	—	—	—	†27.72%	†22.67%	9.83%	9.33%	16.89%	†30.44%	8.78%	†25.72%	16.50%	21.22%	6.61%	14.22%	22.56%
	Ave Rank	7.45	8.76	10.13	7.99	10.27	6.28	7.39	11.49	11.31	10.20	5.41	12.27	7.73	11.40	9.25	14.54	10.59	8.55	

Additionally, a quick look at the win rates reveal that several methods (including Platt scaling) beat the four reference methods simultaneously and with statistical significance. In what follows we conjecture the possible reasons behind this unexpected outcome.

Perhaps the simplest plausible explanation is that we have failed to simulate CS. However, a closer look at these results (and others provided below) disproves this observation. In this regard, we might argue that experiments in which the IID baseline (Platt) fares worse are those affected by a higher degree of CS; indeed this happens prevalently on “yelp→imdb” and “yelp→rt”, for all three classifiers. This seems sensible, as the reviews of the “yelp” domain (about businesses) are topically more different than those from “imdb” or “rt” (which are both about movie reviews). In this respect, it is interesting to see how Head2Tail, CPCS, and TransCal consistently beat the IID baseline, while LasCal (more suitable for LS) instead tends to fare poorly in said cases. That this phenomenon is not also observable when “yelp” acts as the target domain (i.e., in “imdb→yelp” and “rt→yelp”) might be explained by the fact that the “yelp” dataset seems to be the “easiest” problem, in light of the accuracy values obtained by each classifier (reported in A). This characteristic might partially compensate for the effect caused by the shift effect between the distributions.

Concerning the rest of the candidates, all methods seem to perform reasonably well if we rely on the color-coding. However, this impression is misleading, since one method (EMQ^{TransCal}) has obtained extremely poor results (red cells), which skews the color scale and make all other results appear good (i.e., intensely green). This evinces something which is already known in the literature, i.e., that EMQ is extremely sensitive to the quality of the posterior probabilities given as input [Esuli et al., 2021]. In this case, the application of TransCal as a pre-calibration step has lead to huge instabilities in the method. The variant EMQ^{BCTS} instead obtains slightly better results than the vanilla version EMQ; still, all the EMQ variants fall short in terms of performance under CS when compare to other methods. A likely reason is that EMQ is specialised for LS, and its underlying assumptions clash with those of CS. Similar principles likely apply for EMQ^{5B} _{$\rho 2\zeta$} as well.

However, this batch of experiments also offers some unexpected outcomes. Three of the adapted methods, including two adaptations of quantification methods ($PCC_{\rho 2\zeta}^{5B}$, $PACC_{\rho 2\zeta}^{5B}$) and one classifier accuracy predictor ($DoC_{\rho 2\zeta}^{6B}$) have attained the lowest errors overall, as witnessed by the fact that their average ranks appear in bold. It is particularly interesting the case for $PCC_{\rho 2\zeta}^{5B}$, which is an adaptation of the preferred quantifier for CS, and especially for $DoC_{\rho 2\zeta}^{6B}$, which has obtained a much lower error score.

The newly proposed methods do not stand out in terms of performance. PacCal^r shows erratic behavior, with some out-of-scale errors (red cells), while DMCal instead seems to work reasonably well across all datasets, consistently beating at least two reference methods simultaneously in a statistically significant sense.

The results we have obtained for LS are reported in Table 3. In this case, all the reference methods work markedly better than the IID baseline Platt, with LasCal (the only calibration method specifically designed to address this type of shift) standing out by a large margin. None of the direct adaptations seem to be comparable in performance with the reference methods from the calibration literature.

Table 3: Calibration performance under label shift in terms of ECE

		Baselines		Reference				Adapted Methods									
		Platt	Head2Tail	CPCS	TransCal	LasCal	PACC ^{ab} _{0.5}	EMQ ^{ab} _{0.5}	KDEy ^{ab} _{0.5}	ATC ^{ab} _{0.5}	DoC ^{ab} _{0.5}	LEAP ^{ab} _{0.5}	EMQ	EMQ ^{BCTS}	EMQ ^{LasCal}	PacCal ^r	DMCal
Logistic Regression	cmc.3	7.170	5.399	5.390	5.604	4.946	2.692	3.242	3.005	9.067	3.581	2.825	2.138	1.939	10.154	8.835	2.402
	yeast	3.968	4.508	2.374	2.633	1.123	1.686	1.950	2.580	2.581	2.422	2.361	1.342	1.241	8.117	2.780	0.895
	semeion	3.878	3.260	3.133	1.778	2.751	2.682	2.064	2.246	3.672	2.090	2.991	1.120	0.780	1.860	6.419	1.546
	wine-q-red	0.837	1.680	1.036	1.251	1.216	1.837	2.665	2.788	4.456	1.123	2.325	0.886	0.928	0.871	1.363	0.850
	ctg.1	1.055	1.235	1.257	1.143	1.160	1.164	1.405	1.461	3.070	1.347	1.674	0.792	0.802	0.890	2.670	1.034
	ctg.2	2.850	1.496	1.225	1.565	2.818	1.107	1.351	1.432	1.400	2.951	3.904	0.930	1.280	8.032	2.553	0.947
	ctg.3	1.906	2.247	2.353	2.399	1.227	1.899	1.748	1.785	2.367	1.823	1.027	0.790	0.776	1.641	4.490	1.167
	spambase	0.619	0.702	0.707	0.807	0.733	0.725	0.743	0.756	0.775	0.830	0.799	0.685	0.684	0.917	3.906	0.645
	wine-q-white	2.765	2.567	1.946	2.521	1.158	2.170	3.038	3.038	8.086	11.745	2.780	0.728	0.663	3.184	2.223	0.705
	pageblocks.5	14.032	16.249	17.186	12.803	5.085	3.448	2.786	3.063	3.073	2.600	4.270	1.003	1.005	23.808	3.658	2.111
Naive Bayes	cmc.3	7.172	3.260	2.777	3.782	1.921	3.693	3.801	3.750	3.738	5.214	4.887	1.939	2.538	5.527	8.474	3.072
	yeast	11.756	8.269	7.686	35.013	11.353	33.232	33.305	33.188	35.040	35.046	35.047	35.051	35.051	34.711	22.540	35.034
	semeion	17.005	0.145	2.566	4.135	0.662	4.135	3.959	4.007	4.096	4.095	4.097	4.097	4.097	4.101	4.470	4.138
	wine-q-red	1.461	2.223	0.892	4.269	1.155	2.848	2.894	3.370	7.912	1.995	5.136	2.019	4.294	1.493	3.477	1.689
	ctg.1	4.876	3.654	1.608	1.378	2.209	1.602	1.556	1.595	4.255	3.881	2.634	1.791	0.955	2.592	2.974	1.846
	ctg.2	14.101	1.882	2.581	3.978	1.144	3.705	4.004	3.853	4.913	4.905	4.149	4.919	4.919	12.472	4.741	4.229
	ctg.3	10.083	2.500	2.461	3.793	1.212	3.837	3.555	3.534	3.297	3.331	4.585	3.328	3.325	10.541	3.589	3.504
	spambase	3.731	0.689	0.416	2.956	1.259	2.999	3.001	2.985	3.003	3.032	2.911	2.947	2.947	3.858	3.797	2.871
	wine-q-white	5.512	1.133	1.266	1.574	1.359	3.951	4.584	4.447	15.951	10.283	6.316	3.567	0.884	4.129	6.821	1.727
	pageblocks.5	19.648	11.299	8.657	12.111	2.469	10.764	4.740	5.514	10.369	11.328	10.559	3.101	3.095	10.293	10.837	8.327
k Nearest Neighbor	cmc.3	7.734	4.534	4.490	4.448	2.340	6.987	6.986	6.987	16.220	10.285	7.298	2.740	2.911	8.294	12.384	3.408
	yeast	5.608	4.163	2.370	2.539	1.496	3.545	5.019	5.024	6.370	7.510	4.890	1.186	1.186	5.136	3.917	0.789
	semeion	2.422	3.298	3.317	4.476	3.344	2.112	1.165	1.166	8.342	4.639	3.523	0.906	0.918	0.583	6.287	0.464
	wine-q-red	3.673	2.573	1.805	2.526	1.984	3.559	5.661	5.619	4.883	2.016	6.203	1.057	1.071	0.978	3.358	0.755
	ctg.1	4.272	2.334	1.953	1.621	2.428	1.849	2.052	2.005	4.567	3.773	2.587	0.501	0.501	0.653	2.947	0.547
	ctg.2	3.663	3.665	3.141	2.262	2.669	2.554	1.659	1.659	9.223	1.572	1.655	0.426	0.426	0.823	4.973	0.525
	ctg.3	7.073	6.709	6.540	2.523	4.314	3.455	1.701	1.738	5.410	3.716	1.845	0.360	0.361	0.487	6.696	0.714
	spambase	2.116	0.875	0.851	2.182	0.856	0.753	1.453	1.399	2.252	1.085	1.758	0.539	0.542	0.465	2.526	0.462
	wine-q-white	3.861	2.508	2.053	2.749	1.549	4.027	4.919	5.312	17.402	4.830	4.885	1.704	1.704	1.001	4.361	1.046
	pageblocks.5	12.700	12.548	8.424	7.982	3.072	4.869	3.984	4.169	10.166	4.734	7.323	1.648	1.647	1.620	4.520	2.904
Multi-layer Perceptron	cmc.3	4.083	2.668	2.483	3.073	0.768	3.216	3.325	4.451	5.244	4.965	4.971	1.750	1.196	8.724	6.837	1.471
	yeast	4.257	2.322	1.463	1.996	1.029	2.232	2.442	2.566	4.243	3.858	3.818	1.180	0.993	5.834	2.616	1.281
	semeion	2.344	2.400	0.855	1.381	3.308	2.011	1.760	1.904	1.131	1.383	1.019	0.759	0.797	1.744	6.386	0.861
	wine-q-red	1.167	1.767	1.290	1.339	1.240	1.842	2.339	2.519	5.791	1.528	3.520	1.023	1.009	0.879	1.354	1.031
	ctg.1	1.098	1.140	1.560	1.141	1.929	1.096	1.084	1.111	3.350	2.734	1.207	0.654	0.705	1.256	3.217	0.746
	ctg.2	2.980	1.339	1.145	1.713	1.270	1.037	1.005	1.001	1.463	1.229	3.008	0.908	0.857	5.031	2.645	0.964
	ctg.3	1.573	2.333	2.865	1.785	3.153	2.432	1.711	1.898	1.755	2.533	2.270	0.854	0.731	2.768	4.677	2.150
	spambase	0.827	0.773	0.873	0.809	0.916	0.797	0.849	0.795	0.832	0.672	0.722	0.666	0.600	0.999	4.247	0.642
	wine-q-white	1.716	1.366	1.494	1.693	1.077	1.950	2.662	2.756	8.005	3.366	2.797	0.726	0.616	2.139	1.400	0.650
	pageblocks.5	5.829	6.771	7.737	4.464	4.049	4.992	2.162	2.166	4.553	3.968	2.858	0.901	1.031	10.589	5.541	1.980
Wins	Pr(M > 1R)	64.18%	—	—	—	—	71.03%	64.78%	64.00%	51.92%	65.12%	61.48%	†86.02%	†86.98%	72.32%	44.77%	†86.38%
	Pr(M > 2R)	43.75%	—	—	—	—	50.68%	46.75%	45.90%	33.95%	45.82%	42.55%	†69.97%	†42.12%	58.58%	28.40%	†71.55%
	Pr(M > 3R)	28.30%	—	—	—	—	35.98%	35.40%	34.95%	22.90%	31.87%	31.32%	†58.70%	†61.27%	47.02%	17.97%	†59.38%
	Pr(M > 4R)	16.85%	—	—	—	—	20.23%	21.57%	21.25%	11.68%	16.38%	17.57%	†42.43%	†44.32%	33.23%	7.45%	†41.38%
Ave Rank		9.75	8.50	7.31	8.80	7.11	8.79	8.98	9.21	11.28	9.79	10.00	5.71	5.48	7.78	11.71	5.77

As for the rest of the methods, it now appears evident that the EMQ variants dominate. Interestingly enough, EMQ performs better when the classifier being calibrated is Logistic Regression; this is sensible because this classifier is known to be already reasonably well calibrated (for the training distribution), and this is crucial for the method stability [Esuli et al., 2021]. In contrast, for Multilayer Perceptron (which, as a neural approach, is deemed to be overconfident), the pre-calibration round of BCTS seems to improve the results of EMQ. Somehow unexpectedly, though, the variant EMQ_{LasCal} did not improve over vanilla EMQ nor EMQ_{BCTS}, despite relying on a pre-calibration round which is more adapted to this type of shift. Apparently, this method sometimes renders EMQ very unstable (see the many red cells distributed across the column). A likely reason may be that the EMQ requires the original posterior probabilities to be well calibrated for the training distribution, and not for the test distribution. In any case, LasCal alone works reasonably well across all datasets and classifiers, and especially so for Naive Bayes, which is arguably the worst calibrated classifier, and hence the most difficult case.

Another method that stands out in terms of performance, is the newly proposed DMCal, and particularly so for k Nearest Neighbor (perhaps because the already discretized outputs of k -Nearest Neighbors simplify the binning of DMCal). This, together with the fact that (unlike the EMQ variants) DMCal also performed reasonably well under CS, renders this method an interesting versatile approach worth considering in future calibration research related to dataset shift.

Figure 2 show the ECE as a function of level of shift under CS and LS experiments side-by-side for a selection of methods. These figures clearly reveal a natural tendency to degrade the performance as the intensity of shift increases (which indirectly validates the fact that we were indeed generating shift). However, different methods exhibit different degrees of robustness; for example, TransCal and Head2Tail seem to be pretty stable against the intensity of CS, while CPCS and LasCal seem instead to be very unstable in this respect. A comparison between both plots disproves our hypothesis according to which (at least on binary problems) Head2Tail should be more robust to LS than to CS.

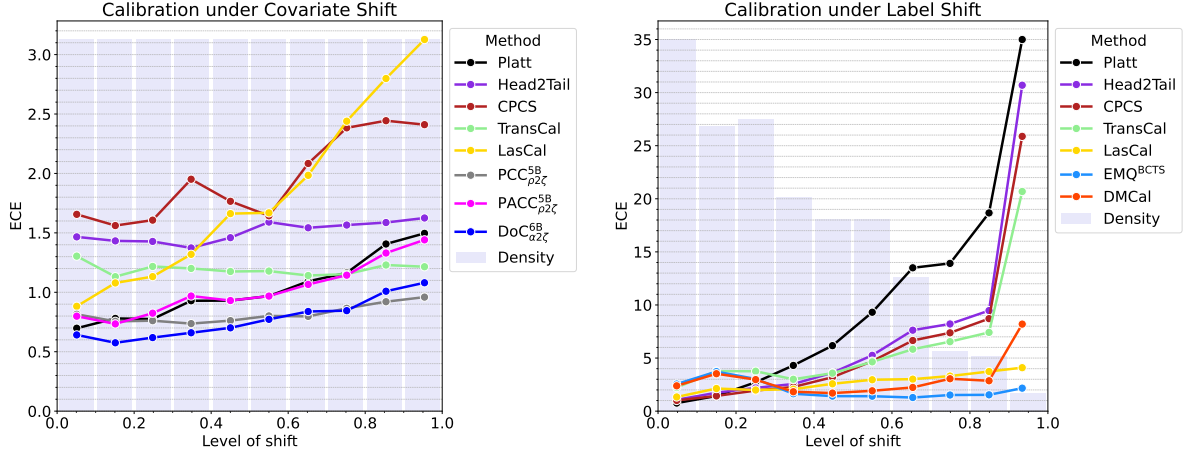


Figure 2: Calibration error in terms of ECE as a function of shift intensity in CS experiments (left panel) and LS (right panel).

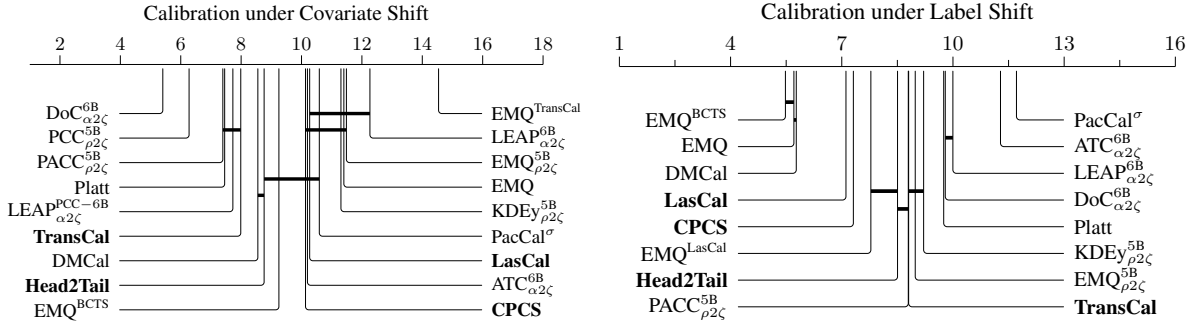


Figure 3: CD-diagrams for CS experiments (left panel) and LS experiments (right panel). Reference calibration methods are highlighted in boldtype.

These plots also reveal that $PCC_{\rho 2\zeta}^{5B}$ seems preferable to $DoC_{\alpha 2\zeta}^{6B}$ when the level of CS is extremely high. Similarly interesting is the fact that $PACC_{\rho 2\zeta}^{5B}$ (a non-parametric calibrator) behaves very similarly to Platt scaling (a parametric one), somehow suggesting that the calibration maps both methods find out tend to be very similar. In terms of LS (right panel), it is interesting to see how LasCal, EMQ^{BCTS} and (to a lesser extent) DMCal behave very robustly against the intensity of the shift.

The CD-diagrams (Figure 3) confirm that $DoC_{\alpha 2\zeta}^{6B}$ and $PCC_{\rho 2\zeta}^{5B}$ fare significantly better than the competitors under CS, while EMQ^{BCTS} , EMQ, and the newly proposed DMCal seem to dominate the LS arena, followed by LasCal.

These results are interesting, since they clearly show how different techniques from quantification and classifier accuracy prediction can be effectively used in the calibration field yielding unexpected success. Notwithstanding this, one might argue that ECE does not tell the whole story, since some of the calibration methods we propose are not guaranteed to be accuracy-preserving (i.e., in the process of calibrating the posteriors, they may well shift the decision boundary in the calibration map). In Tables 10 and 11 (in the Appendix), we report Brier Scores values for CS and LS, respectively. These results reveal that low ECE has not come at the cost of accuracy (i.e., the best performing methods in terms of ECE also tend to perform well in terms of Brier Score), with the sole exception of LasCal under LS, which drops some positions in the average ranking.

6.4.2 Quantification Experiments

In this section, we report the results we have obtained for the task of quantification. The evaluation measure we adopt is the absolute error (AE) [Sebastiani, 2020], given by:

$$AE = |p - \hat{p}| \quad (32)$$

where $p \in [0, 1]$ is the true prevalence value of the positive class, and $\hat{p} \in [0, 1]$ is the estimated prevalence value obtained by the quantification method.

In this case, we consider PACC, EMQ, and KDEy as our reference methods, and apply the $\alpha 2\rho$ and $\zeta 2\rho$ adaptation algorithms to generate new quantification methods from classifier accuracy predictors and calibrators, respectively. When the type of shift is CS, we also include PCC as an additional reference quantification method, and we also consider $LEAP_{\alpha 2\rho}^{PCC}$, an adaptation of LEAP equipped with PCC as the surrogate quantifier. For LS experiments, we also consider EMQ^{BCTS} as an additional reference method. The IID baseline is CC, a method that simply classifies and counts the fraction of predicted positive instances in the test set. We do not consider adaptations from $PacCal^\sigma$ nor $DMCal$, since those methods heavily rely on quantification methods and would therefore be redundant to the comparison.

Table 4 reports the results for CS simulations. As expected, PCC is the top-performing reference quantifier; the rest of the proper quantification methods (PACC, EMQ, KDEy) fall short in terms of AE given that the underlying assumptions on which these methods rely upon do not align well with the characteristics of the data (see also [González et al., 2024]). Indeed, the IID baseline (CC) tends to outperform three methods (presumably PACC, EMQ, and KDEy) consistently and with statistical significance (see the win rates).

All the newly proposed methods, with the sole exception of $LEAP_{\alpha 2\rho}$ (which internally relies on KDEy) perform better than the reference methods PACC, EMQ, and KDEy in most cases. The top performing methods overall include $DoC_{\alpha 2\rho}$, the proposed variant $LEAP_{\alpha 2\rho}^{PCC}$, and $TransCal_{\zeta 2\rho}$. This is interesting for a number of reasons. The first one is that, together with the calibration experiments, DoC gets consolidated as a versatile method for CS problems. Second, because a variant of LEAP equipped with PCC is something that has never been investigated in past literature and, when adapted to quantification via the $\alpha 2\rho$ method, it seems to work even better than vanilla PCC; LEAP is based on the resolution of a system of linear equations representing problem constraints, which may help improve the stability of the method. Third and foremost, because $TransCal_{\zeta 2\rho}$ has attained astonishing unexpected results, clearly

Table 4: Quantification performance under CS in terms of AE

		Baselines	Reference				Adapted Methods						
		CC	PCC	PACC	EMQ	KDEy	$ATC_{\alpha 2\rho}$	$DoC_{\alpha 2\rho}$	$LEAP_{\alpha 2\rho}$	$LEAP_{\alpha 2\rho}^{PCC}$	$CPCS_{\zeta 2\rho}$	$TransCal_{\zeta 2\rho}$	$LasCal_{\zeta 2\rho}$
BERT	imdb→rt	0.045	0.027	0.123	0.131	0.149	0.065	0.043	0.151	0.027	0.038	0.025	0.031
	imdb→yelp	0.072	0.037	0.068	0.182	0.073	0.042	0.031	0.130	0.037	0.053	0.029	0.047
	rt→imdb	0.075	0.031	0.143	0.367	0.161	0.047	0.034	0.169	0.031	0.057	0.027	0.038
	rt→yelp	0.032	0.027	0.078	0.120	0.107	0.034	0.028	0.306	0.027	0.028	0.029	0.027
	yelp→imdb	0.112	0.083	0.137	0.164	0.148	0.094	0.094	0.160	0.083	0.101	0.040	0.091
	yelp→rt	0.100	0.074	0.120	0.154	0.140	0.093	0.084	0.135	0.074	0.087	0.035	0.082
DistilBERT	imdb→rt	0.036	0.036	0.051	0.056	0.053	0.038	0.035	0.066	0.036	0.033	0.024	0.033
	imdb→yelp	0.019	0.022	0.025	0.027	0.024	0.024	0.020	0.044	0.022	0.019	0.023	0.019
	rt→imdb	0.057	0.033	0.045	0.062	0.047	0.031	0.030	0.072	0.033	0.038	0.028	0.040
	rt→yelp	0.094	0.064	0.125	0.131	0.112	0.062	0.056	0.154	0.064	0.057	0.034	0.073
	yelp→imdb	0.099	0.083	0.102	0.133	0.112	0.084	0.067	0.116	0.083	0.086	0.039	0.085
	yelp→rt	0.083	0.068	0.081	0.112	0.090	0.067	0.051	0.091	0.068	0.058	0.032	0.071
RoBERTa	imdb→rt	0.097	0.073	0.130	0.160	0.150	0.076	0.080	0.140	0.073	0.081	0.038	0.079
	imdb→yelp	0.019	0.017	0.018	0.019	0.018	0.021	0.016	0.047	0.017	0.019	0.023	0.017
	rt→imdb	0.109	0.072	0.233	0.207	0.187	0.108	0.076	0.193	0.072	0.075	0.040	0.081
	rt→yelp	0.099	0.064	0.221	0.201	0.179	0.102	0.067	0.196	0.064	0.063	0.035	0.071
	yelp→imdb	0.041	0.037	0.055	0.053	0.061	0.047	0.048	0.072	0.037	0.038	0.024	0.037
	yelp→rt	0.027	0.023	0.019	0.042	0.021	0.021	0.017	0.044	0.023	0.023	0.020	0.022
Wins	$Pr(M > 1R)$	†90.56%	—	—	—	—	†89.89%	†96.17%	54.28%	†95.50%	†93.78%	†88.67%	†95.83%
	$Pr(M > 2R)$	†75.00%	—	—	—	—	†81.39%	†88.06%	40.11%	†85.56%	†82.44%	†84.94%	†84.28%
	$Pr(M > 3R)$	†64.06%	—	—	—	—	†72.83%	†79.44%	30.33%	†77.33%	†73.22%	†76.94%	†76.11%
	$Pr(M > 4R)$	14.06%	—	—	—	—	†29.17%	†36.50%	12.28%	†39.72%	†27.39%	†62.78%	18.06%
	Ave Rank	7.28	4.69	8.12	9.84	8.52	5.94	4.72	9.40	4.64	5.68	3.66	5.52

Table 5: Quantification performance under label shift in terms of AE

		Baselines	Reference				Adapted Methods							
		CC	PACC	EMQ	EMQ ^{BCTS}	KDEy	ATC _{α_{2p}}	DoC _{α_{2p}}	LEAP _{α_{2p}}	CPCS _{ζ_{2p}}	TransCal _{ζ_{2p}}	LasCal _{ζ_{2p}}	Head2Tail _{ζ_{2p}}	EMQ ^{LasCal}
Logistic Regression	cmc.3	0.323	0.117	0.122	0.105	0.112	0.238	0.090	0.198	0.243	0.244	0.208	0.245	0.251
	yeast	0.239	0.079	0.109	0.074	0.060	0.192	0.090	0.092	0.201	0.223	0.162	0.212	0.217
	semeion	0.134	0.028	0.033	0.009	0.026	0.093	0.026	0.025	0.127	0.198	0.125	0.122	0.091
	wine-q-red	0.126	0.044	0.038	0.041	0.044	0.160	0.077	0.078	0.179	0.214	0.178	0.204	0.039
	ctg.1	0.084	0.033	0.015	0.015	0.015	0.082	0.030	0.032	0.110	0.176	0.118	0.114	0.025
	ctg.2	0.150	0.055	0.016	0.048	0.030	0.210	0.032	0.025	0.178	0.205	0.146	0.187	0.214
	ctg.3	0.123	0.024	0.010	0.010	0.022	0.082	0.072	0.095	0.123	0.175	0.129	0.125	0.096
	spambase	0.043	0.015	0.015	0.015	0.013	0.049	0.029	0.020	0.066	0.162	0.062	0.082	0.031
	wine-q-white	0.232	0.047	0.041	0.035	0.041	0.193	0.068	0.062	0.213	0.226	0.201	0.219	0.130
	pageblocks.5	0.339	0.034	0.045	0.045	0.046	0.213	0.068	0.060	0.339	0.213	0.168	0.324	0.412
Naïve Bayes	cmc.3	0.241	0.111	0.091	0.106	0.115	0.174	0.119	0.119	0.224	0.236	0.202	0.231	0.161
	yeast	0.508	0.336	0.508	0.508	0.336	0.170	0.238	0.518	0.249	0.218	0.279	0.252	0.505
	semeion	0.100	0.102	0.100	0.100	0.100	0.097	0.232	0.527	0.131	0.206	0.157	0.168	0.100
	wine-q-red	0.141	0.068	0.103	0.130	0.063	0.162	0.156	0.184	0.194	0.211	0.193	0.222	0.066
	ctg.1	0.112	0.024	0.059	0.019	0.020	0.098	0.052	0.028	0.125	0.173	0.133	0.179	0.100
	ctg.2	0.122	0.044	0.128	0.128	0.036	0.168	0.145	0.350	0.187	0.200	0.159	0.194	0.273
	ctg.3	0.153	0.036	0.140	0.140	0.027	0.110	0.133	0.271	0.139	0.181	0.137	0.145	0.256
	spambase	0.119	0.024	0.119	0.119	0.024	0.085	0.196	0.341	0.141	0.173	0.155	0.153	0.104
	wine-q-white	0.195	0.063	0.125	0.054	0.063	0.202	0.113	0.093	0.211	0.220	0.206	0.223	0.207
	pageblocks.5	0.282	0.043	0.131	0.131	0.076	0.223	0.162	0.368	0.216	0.217	0.160	0.274	0.263
k Nearest Neighbor	cmc.3	0.319	0.094	0.128	0.128	0.108	0.210	0.109	0.165	0.231	0.241	0.184	0.238	0.209
	yeast	0.246	0.094	0.064	0.064	0.059	0.219	0.052	0.055	0.199	0.219	0.183	0.202	0.172
	semeion	0.172	0.015	0.012	0.012	0.012	0.056	0.045	0.072	0.151	0.205	0.155	0.154	0.016
	wine-q-red	0.144	0.056	0.070	0.070	0.054	0.155	0.101	0.165	0.194	0.220	0.201	0.214	0.056
	ctg.1	0.122	0.041	0.017	0.017	0.023	0.074	0.026	0.023	0.147	0.186	0.151	0.146	0.020
	ctg.2	0.228	0.072	0.017	0.017	0.031	0.156	0.028	0.027	0.176	0.201	0.139	0.182	0.032
	ctg.3	0.219	0.036	0.017	0.017	0.018	0.098	0.021	0.018	0.188	0.193	0.166	0.189	0.017
	spambase	0.080	0.017	0.020	0.020	0.016	0.059	0.031	0.022	0.090	0.174	0.091	0.096	0.021
	wine-q-white	0.172	0.044	0.098	0.098	0.042	0.176	0.154	0.217	0.206	0.221	0.196	0.210	0.052
	pageblocks.5	0.351	0.031	0.107	0.107	0.059	0.217	0.094	0.082	0.252	0.213	0.142	0.304	0.088
Multi-layer Perceptron	cmc.3	0.218	0.083	0.092	0.062	0.070	0.203	0.154	0.163	0.222	0.232	0.191	0.227	0.328
	yeast	0.195	0.046	0.063	0.044	0.046	0.213	0.102	0.101	0.199	0.219	0.179	0.202	0.202
	semeion	0.075	0.020	0.010	0.009	0.014	0.046	0.023	0.024	0.079	0.189	0.084	0.079	0.056
	wine-q-red	0.119	0.040	0.054	0.037	0.036	0.163	0.082	0.064	0.176	0.207	0.177	0.197	0.042
	ctg.1	0.082	0.018	0.016	0.011	0.012	0.096	0.024	0.036	0.103	0.168	0.107	0.106	0.053
	ctg.2	0.181	0.037	0.053	0.033	0.036	0.180	0.079	0.126	0.182	0.202	0.156	0.187	0.190
	ctg.3	0.112	0.026	0.010	0.020	0.041	0.083	0.158	0.138	0.110	0.170	0.118	0.111	0.109
	spambase	0.039	0.014	0.016	0.016	0.014	0.050	0.027	0.022	0.060	0.153	0.051	0.060	0.035
	wine-q-white	0.172	0.033	0.034	0.030	0.029	0.156	0.068	0.072	0.192	0.214	0.185	0.191	0.072
	pageblocks.5	0.219	0.029	0.029	0.029	0.022	0.148	0.059	0.038	0.213	0.191	0.177	0.204	0.248
Wins	Pr($M \succ 1R$)	25.47%	—	—	—	—	32.30%	54.67%	48.98%	25.45%	20.95%	31.40%	23.15%	49.33%
	Pr($M \succ 2R$)	21.43%	—	—	—	—	27.27%	43.43%	38.70%	21.10%	17.55%	25.97%	19.48%	39.40%
	Pr($M \succ 3R$)	11.10%	—	—	—	—	14.88%	26.52%	23.33%	12.40%	10.12%	14.60%	11.35%	21.70%
	Pr($M \succ 4R$)	7.72%	—	—	—	—	10.47%	16.75%	14.17%	8.20%	6.42%	9.65%	7.83%	13.45%
Ave Rank		9.04	4.50	4.87	4.59	4.09	7.60	6.10	6.90	8.96	9.72	8.14	9.51	6.98

beating any other method from the pool consistently and across all classifiers. The fact that TransCal performed comparatively better in quantification experiments than in calibration ones might be an indication that its post-hoc calibrated posteriors are better calibrated at the dataset level (i.e., in terms of overall expected bias) rather than at the bin level (i.e., are less informative at a finer-grained level). This suggests the inner workings of TransCal, based on importance weighting, deserve closer investigation for quantification under CS.

The quantification experiments under LS are reported in Table 5. In this case, there are no surprises: the reference quantification methods clearly dominate the experimental comparison, with KDEy standing as the top performer of the lot (this is in line with the results of [Moreo et al., 2025]). Among the adapted methods, the best performer is DoC _{α_{2p}} . Although not comparable in performance with respect to the reference methods, it is interesting to note that DoC keeps performing reasonably well across different tasks and types of shift.

Figure 4 show the “errors-by-shift” plots of quantification experiments, side-by-side for both types of shift, for a selection of methods. Interestingly enough, TransCal _{ζ_{2p}} is not only the best performer under CS, but is also the most robust to the intensity of this shift. The rest of the methods’ performance suffer when the level of CS increases.

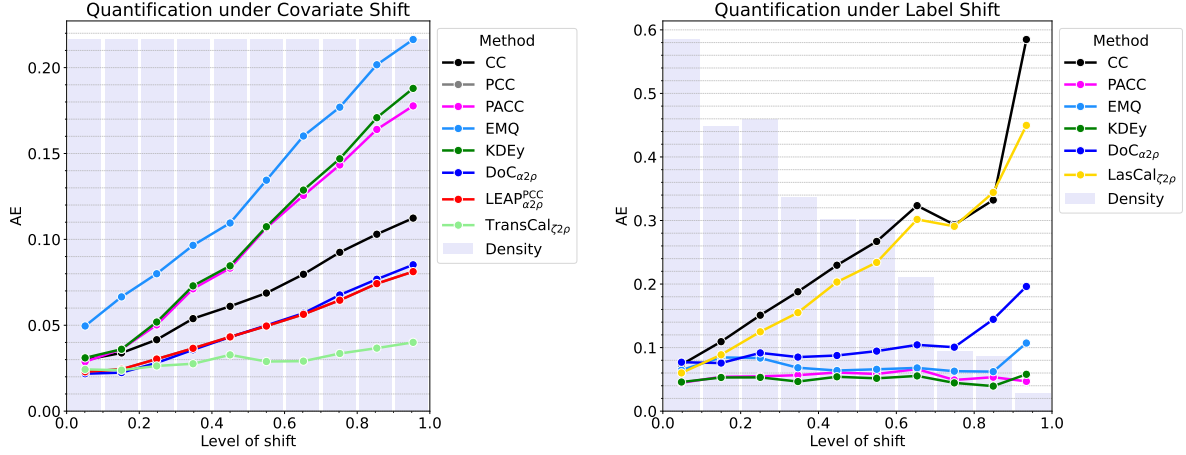


Figure 4: Quantification error in terms of AE as a function of shift intensity in CS experiments (left panel) and LS (right panel).

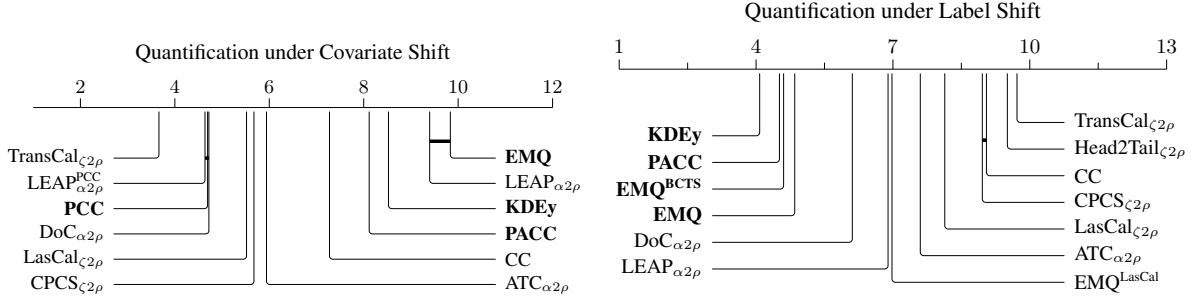


Figure 5: CD-diagrams for CS experiments (left panel) and LS experiments (right panel). Reference quantification methods are highlighted in boldtype.

Concerning the level of LS, not only the three reference methods PACC, EMQ, and KDEy, but also the new adaptation DoC $\alpha_{2\rho}$, seem to be pretty robust against it. Despite the fact that LasCal is designed to counter LS, its performance degrades notably as the intensity of the shift increases.

Figure 5 display the CD-diagrams for the quantification experiments for both types of shift side by side. It is interesting to see how TransCal $\zeta_{2\rho}$ dominates the rank for CS in isolation, i.e., without being included in any critical difference group. The same plot reveals LEAP $\alpha_{2\rho}^{\text{PCC}}$ and DoC $\alpha_{2\rho}$ are very close to each other, in a statistically significant sense, to PCC under CS. By comparing the CD-diagrams for both types of shift, it is interesting to see how these are almost specular, i.e., the best performing methods for CS are among the worst performing methods for LS, and viceversa (see, e.g., TransCal $\zeta_{2\rho}$). This looks like an indication that, in order to make an informed decision about which method to use, we should be pretty sure about the type of shift at play, which in turn suggests more research on dataset shift detection [Rabanser et al., 2019] urges. A notable exception to this phenomenon is DoC $\alpha_{2\rho}$ which occupies a relatively high rank in both types of shift.

6.4.3 Classifier Accuracy Prediction Experiments

We now turn to discussing the results we have obtained for classifier accuracy prediction. The evaluation measure we adopt is the Absolute estimation Error (AE) [Garg et al., 2022], given by:

$$AE = |\text{Acc} - \hat{\text{Acc}}| \quad (33)$$

between the true accuracy (Acc) and the estimated accuracy ($\hat{\text{Acc}}$). As our measure of classifier accuracy, we consider vanilla accuracy, i.e., the proportion of correctly classified instances. We report mean scores of AE averaged across all test samples generated for each dataset.

We confront our reference methods ATC, DoC, and LEAP against direct adaptations of the reference methods from quantification and calibration. The IID baseline (Naive) is a method that, regardless of the test set, reports the accuracy estimated in the validation set. In CS experiments, we additionally consider LEAP^{PCC} as a reference method, and PCC _{$\rho_{2\alpha}$} as an adaptation method. In this case, we also experiment with DMCal _{$\zeta_{2\alpha}$} , an adaptation of the newly proposed DMcal method which in the experiments of Section 6.4.1 showed promising performance for calibration.

Table 6 reports the experimental results we have obtained for CS. The reference methods tend to dominate the experimental comparison, with DoC performing very well once again. Somehow surprisingly, though, LEAP^{PCC} did not perform better than LEAP notwithstanding the fact that PCC should be more reliable than KDEy as an underlying quantifier under CS. Conversely, the adaptation PCC _{$\rho_{2\alpha}$} is one of the best performing systems of the experimental comparison. EMQ _{$\rho_{2\alpha}$} behaves unstably, but the pre-calibration round of EMQ _{$\rho_{2\alpha}$} ^{BCTS} seems to partially compensate for it. TransCal _{$\zeta_{2\alpha}$} is one of the worst performing systems of the lot. This was not to be expected given that, under CS, it showed excellent quantification performance. However, this partially corroborates our hypothesis that the calibrated posteriors of TransCal _{$\zeta_{2\alpha}$} are not very informative from a finer-grained perspective, i.e., that when we separately inspect the posteriors assigned to the predicted positives and the predicted negatives (as is the rationale behind $\zeta_{2\alpha}$), these do not locally reflect the model’s uncertainty well. It is also surprising that, among all the calibration adaptations, LasCal _{$\zeta_{2\alpha}$} , a method addressing LS, works best.

Table 7 reports the AE results under LS. Also in this case, the reference methods achieve superior performance. The best performing system is LEAP, closely followed by DoC. The adaptation methods show erratic behavior, sometimes achieving very good results and sometimes failing loudly.

Figure 6 show the AE as a function of the level of shift for a selection of methods. Most methods improve over the naive baseline, with the exception of LEAP^{PCC} (left panel) which becomes progressively unreliable as the level of

Table 6: Classifier accuracy prediction under CS in terms of AE

		Baselines	Reference				Adapted Methods								
		Naive	ATC	DoC	LEAP	LEAP ^{PCC}	PCC _{$\rho_{2\alpha}$}	PACC _{$\rho_{2\alpha}$}	EMQ _{$\rho_{2\alpha}$}	EMQ ^{BCTS} _{$\rho_{2\alpha}$}	KDEy _{$\rho_{2\alpha}$}	CPCS _{$\zeta_{2\alpha}$}	TransCal _{$\zeta_{2\alpha}$}	LasCal _{$\zeta_{2\alpha}$}	DMCal _{$\zeta_{2\alpha}$}
BERT	imdb→rt	0.044	0.033	0.032	0.037	0.042	0.053	0.129	0.722	0.128	0.157	0.117	0.130	0.036	0.120
	imdb→yelp	0.026	0.027	0.022	0.027	0.041	0.068	0.071	0.722	0.073	0.084	0.087	0.150	0.043	0.059
	rt→imdb	0.024	0.032	0.024	0.026	0.060	0.091	0.082	0.696	0.079	0.124	0.118	0.142	0.038	0.105
	rt→yelp	0.024	0.031	0.021	0.031	0.039	0.089	0.096	0.689	0.095	0.104	0.106	0.137	0.051	0.149
	yelp→imdb	0.076	0.053	0.058	0.068	0.113	0.039	0.041	0.261	0.045	0.048	0.105	0.090	0.060	0.035
	yelp→rt	0.094	0.058	0.066	0.081	0.128	0.044	0.067	0.339	0.074	0.060	0.109	0.084	0.070	0.040
DistiBERT	imdb→rt	0.047	0.038	0.038	0.048	0.038	0.037	0.044	0.047	0.045	0.055	0.066	0.071	0.063	0.040
	imdb→yelp	0.017	0.020	0.016	0.018	0.020	0.017	0.041	0.043	0.041	0.054	0.046	0.111	0.023	0.038
	rt→imdb	0.026	0.038	0.027	0.032	0.036	0.030	0.125	0.200	0.123	0.122	0.054	0.124	0.037	0.092
	rt→yelp	0.025	0.029	0.029	0.030	0.051	0.020	0.086	0.064	0.081	0.096	0.071	0.098	0.048	0.080
	yelp→imdb	0.070	0.044	0.039	0.066	0.089	0.039	0.069	0.123	0.078	0.049	0.060	0.067	0.058	0.036
	yelp→rt	0.099	0.070	0.059	0.097	0.114	0.060	0.073	0.146	0.094	0.057	0.075	0.052	0.086	0.040
RoBERTa	imdb→rt	0.081	0.039	0.056	0.091	0.043	0.045	0.095	0.177	0.112	0.082	0.089	0.066	0.077	0.068
	imdb→yelp	0.020	0.021	0.019	0.021	0.022	0.027	0.038	0.093	0.041	0.049	0.059	0.130	0.018	0.034
	rt→imdb	0.025	0.054	0.041	0.028	0.063	0.024	0.159	0.139	0.157	0.160	0.064	0.093	0.042	0.116
	rt→yelp	0.026	0.045	0.031	0.029	0.052	0.026	0.137	0.148	0.136	0.140	0.061	0.108	0.037	0.101
	yelp→imdb	0.054	0.026	0.034	0.044	0.068	0.019	0.083	0.289	0.096	0.055	0.028	0.093	0.032	0.049
	yelp→rt	0.113	0.026	0.057	0.099	0.111	0.024	0.254	0.459	0.304	0.253	0.053	0.081	0.049	0.161
Wins	Pr($M > 1R$)	†87.22%	—	—	—	—	75.67%	42.67%	17.89%	42.00%	42.78%	54.61%	30.39%	74.17%	47.94%
	Pr($M > 2R$)	53.06%	—	—	—	—	64.17%	30.89%	11.83%	29.00%	31.83%	39.00%	23.61%	53.28%	36.56%
	Pr($M > 3R$)	31.56%	—	—	—	—	52.67%	23.06%	9.50%	21.67%	24.72%	27.83%	17.50%	32.06%	28.83%
	Pr($M > 4R$)	14.83%	—	—	—	—	31.89%	16.17%	5.78%	14.56%	17.11%	13.89%	12.00%	15.28%	22.11%
Ave Rank		6.18	5.03	4.70	6.13	7.35	5.15	8.70	12.08	9.02	8.76	8.02	10.01	6.40	7.46

Table 7: Classifier accuracy prediction under label shift in terms of AE

		Baselines	Reference			Adapted Methods						
		Naive	ATC	DoC	LEAP	PACC $_{\rho 2\alpha}$	EMQ $_{\rho 2\alpha}$	KDEy $_{\rho 2\alpha}$	CPCS $_{\zeta 2\alpha}$	TransCal $_{\zeta 2\alpha}$	LasCal $_{\zeta 2\alpha}$	DMCal $_{\zeta 2\alpha}$
Logistic Regression	cmc.3	0.178	0.149	0.074	0.076	0.104	0.147	0.141	0.156	0.168	0.169	0.095
	yeast	0.130	0.088	0.047	0.048	0.051	0.057	0.067	0.103	0.095	0.114	0.065
	semeion	0.119	0.088	0.035	0.041	0.023	0.028	0.031	0.110	0.074	0.090	0.040
	wine-q-red	0.021	0.060	0.023	0.022	0.093	0.066	0.089	0.040	0.087	0.028	0.099
	ctg.1	0.041	0.022	0.023	0.018	0.026	0.040	0.030	0.018	0.081	0.020	0.027
	ctg.2	0.097	0.072	0.093	0.125	0.032	0.041	0.030	0.057	0.038	0.030	0.047
	ctg.3	0.105	0.021	0.041	0.028	0.057	0.132	0.042	0.078	0.045	0.058	0.028
	spambase	0.018	0.017	0.014	0.017	0.037	0.063	0.027	0.034	0.057	0.023	0.026
	wine-q-white	0.120	0.094	0.045	0.039	0.066	0.110	0.075	0.082	0.080	0.130	0.092
	pageblocks.5	0.326	0.122	0.049	0.031	0.053	0.046	0.055	0.300	0.232	0.248	0.080
Naïve Bayes	cmc.3	0.092	0.059	0.042	0.042	0.113	0.257	0.097	0.064	0.086	0.091	0.142
	yeast	0.273	0.159	0.226	0.325	0.241	0.523	0.513	0.238	0.370	0.242	0.522
	semeion	0.027	0.185	0.051	0.040	0.314	0.201	0.306	0.136	0.199	0.096	0.201
	wine-q-red	0.035	0.028	0.031	0.049	0.074	0.264	0.075	0.025	0.103	0.027	0.107
	ctg.1	0.062	0.040	0.027	0.015	0.038	0.137	0.061	0.020	0.038	0.030	0.106
	ctg.2	0.068	0.023	0.036	0.029	0.115	0.200	0.143	0.130	0.149	0.130	0.180
	ctg.3	0.119	0.032	0.136	0.050	0.208	0.167	0.069	0.072	0.147	0.035	0.149
	spambase	0.055	0.055	0.051	0.019	0.163	0.157	0.235	0.061	0.146	0.148	0.152
	wine-q-white	0.081	0.040	0.047	0.038	0.121	0.348	0.124	0.029	0.103	0.070	0.172
	pageblocks.5	0.272	0.025	0.067	0.045	0.076	0.173	0.049	0.199	0.229	0.195	0.229
k Nearest Neighbor	cmc.3	0.175	0.225	0.075	0.069	0.171	0.084	0.166	0.147	0.155	0.175	0.123
	yeast	0.130	0.102	0.047	0.099	0.061	0.174	0.063	0.114	0.100	0.119	0.053
	semeion	0.141	0.080	0.026	0.015	0.123	0.317	0.097	0.086	0.026	0.081	0.089
	wine-q-red	0.029	0.146	0.031	0.028	0.112	0.086	0.142	0.046	0.072	0.042	0.104
	ctg.1	0.072	0.108	0.026	0.021	0.023	0.060	0.028	0.046	0.040	0.055	0.025
	ctg.2	0.162	0.177	0.036	0.098	0.027	0.045	0.033	0.060	0.064	0.079	0.030
	ctg.3	0.194	0.119	0.033	0.036	0.019	0.122	0.020	0.160	0.091	0.138	0.019
	spambase	0.040	0.070	0.018	0.024	0.030	0.078	0.030	0.043	0.073	0.029	0.039
	wine-q-white	0.076	0.032	0.030	0.031	0.134	0.133	0.164	0.037	0.044	0.065	0.098
	pageblocks.5	0.336	0.232	0.029	0.036	0.059	0.107	0.071	0.248	0.218	0.247	0.131
Multi-layer Perceptron	cmc.3	0.128	0.083	0.047	0.039	0.164	0.303	0.172	0.104	0.114	0.118	0.117
	yeast	0.089	0.051	0.054	0.055	0.087	0.192	0.138	0.057	0.063	0.078	0.069
	semeion	0.083	0.015	0.015	0.018	0.042	0.165	0.021	0.079	0.036	0.051	0.020
	wine-q-red	0.037	0.029	0.035	0.021	0.112	0.164	0.102	0.021	0.086	0.028	0.087
	ctg.1	0.060	0.034	0.022	0.013	0.022	0.038	0.033	0.026	0.022	0.043	0.058
	ctg.2	0.116	0.027	0.107	0.073	0.163	0.084	0.129	0.042	0.033	0.066	0.066
	ctg.3	0.100	0.056	0.026	0.025	0.030	0.033	0.051	0.085	0.047	0.073	0.050
	spambase	0.020	0.019	0.015	0.016	0.056	0.045	0.033	0.024	0.021	0.030	0.030
	wine-q-white	0.077	0.054	0.027	0.024	0.066	0.059	0.068	0.049	0.040	0.071	0.082
	pageblocks.5	0.225	0.139	0.069	0.053	0.048	0.042	0.041	0.108	0.105	0.141	0.059
Wins	Pr($M > 1R$)	46.33%	—	—	—	55.77%	39.88%	56.55%	63.42%	51.75%	55.15%	54.43%
	Pr($M > 2R$)	26.97%	—	—	—	35.48%	21.40%	34.83%	34.27%	25.32%	30.90%	30.80%
	Pr($M > 3R$)	12.07%	—	—	—	19.82%	11.82%	19.07%	16.32%	12.90%	15.43%	16.12%
	Ave Rank	7.15	5.65	4.17	4.05	5.97	7.91	6.12	5.79	6.58	6.20	6.42

shift increases. None of the methods, however, are able to compensate for higher levels of CS, suggesting that further research is needed. Concerning the experiments of LS, LEAP and PACC $_{\rho 2\alpha}$ are very stable even at high levels of prior shift. The rest of the methods, including DoC, perform worse at higher levels of prior shift.

The CD-diagrams (Figure 7) reveal that, under CS, the top-performing methods DoC, ATC, and PCC $_{\rho 2\alpha}$ are actually not significantly different from each other, and that LEAP and LasCal $_{\zeta 2\alpha}$ are not better than the Naive baseline. In LS, LEAP stands out over DoC and ATC, which nevertheless perform better than the rest of the methods. Only EMQ $_{\rho 2\alpha}$ proves inferior than the Naive baseline under prior shift.

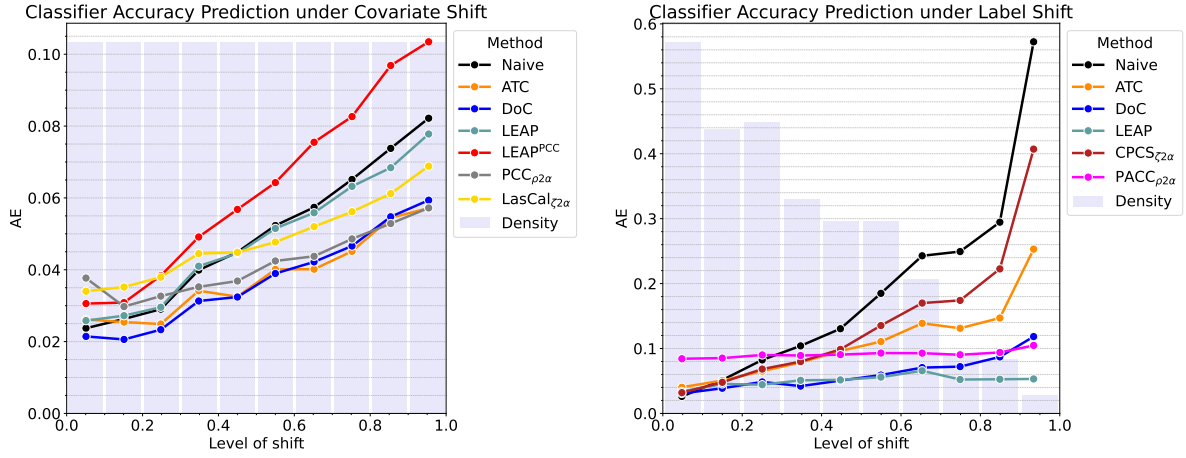


Figure 6: Classifier accuracy prediction error in terms of AE as a function of shift intensity in CS experiments (left panel) and LS (right panel).

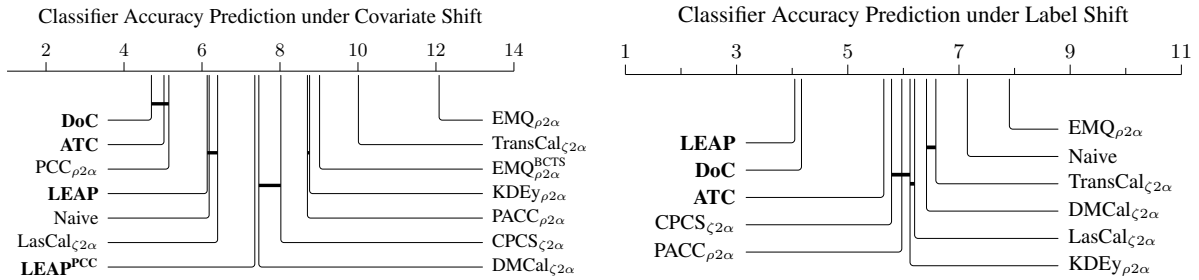


Figure 7: CD-diagrams for CS experiments (left panel) and LS experiments (right panel). Reference classifier accuracy prediction methods are highlighted in boldtype.

7 Conclusions

In this paper, we have investigated the interconnections between calibration, quantification, and classifier accuracy prediction under dataset shift, showing that these problems are close to each other, to the extent that methods originally proposed for one of the problems can be adapted to address the other problems. We have first provided formal proofs of the reduction of one problem to another based on the availability of perfect oracles. Building on these proofs, we have designed practical adaptation methods which we have tested experimentally. Additionally, we have proposed two new calibration methods, PacCal^r and DMCal, that leverage consolidated principles that render quantification methods robust to LS conditions.

Our experiments have led to several interesting (and sometimes unexpected) findings. Among the three tasks considered, calibration appears to benefit the most from the adaptation of methods originally proposed for quantification and classifier accuracy prediction. This may seem counter-intuitive at first glance, given that calibration is the most long-standing field among the three. However, the specific branch of calibration on which this paper focuses (i.e., calibration under dataset shift) is relatively recent [Ovadia et al., 2019]. In this respect, the newly proposed DMCal, which builds on ideas from the quantification literature, has shown strong potential for calibration under both CS and, especially, LS.

Conversely, quantification and classifier accuracy prediction have benefited less from the adaptation of methods from the other tasks and particularly so when confronting LS, where native state-of-the-art approaches from their respective fields still stand out in terms of performance. Notwithstanding this, the adaptation of one calibration method, TransCal, has surprisingly emerged as the top-performing method for quantification under CS conditions in our experiments. Further experiments involving different data sources and alternative protocols for simulating CS may provide further evidence that confirm or refute this finding.

We have observed that EMQ tends to stand out as one of the best-performing methods overall in both quantification and calibration problems. However, it often presents stability issues that hinder its effectiveness. Introducing a calibration phase before the application of the EM algorithm can help mitigate this effect, but in certain cases it may even prove counterproductive. More research is needed in order to better understand the conditions under which introducing a calibration phase is beneficial, and to explore whether it is possible to automatically select the most appropriate calibrator to use depending on the type of shift.

Perhaps one of the most surprising outcomes of our experiments is the unexpectedly good performance that DoC, a method originally proposed for classifier accuracy prediction, has consistently shown across all three tasks, and across both types of shift, in most cases. A key component of DoC is the internal sampling generation protocol used for generating validation samples with which a regressor is trained. One may (maybe legitimately) argue that our variants of DoC benefit from a certain advantage over the rest, as they rely on different sampling generation protocols depending on the type of shift. However, given the potential the method has showcased across all tasks and types of shift, we rather believe this is a strong indication that the inner workings of DoC deserve further attention. We foresee the key components for attaining a unified approach to the three problems will revolve around: (i) devising effective methods for detecting the type of shift at play [Rabanser et al., 2019], (ii) devising effective protocols for generating validation samples representative of that particular type of shift [González et al., 2024], and (iii) investigating more effective ways to train a task-specific regressor [Guillory et al., 2021, Pérez-Mon et al., 2025].

Something our experiments seem to indicate, though, is that no single method consistently outperforms the others across all problems and regardless of the type of dataset shift. In future research, it would be interesting to better characterize the relative merits of each method with respect to specific types (and ideally even with respect to the level of intensity) of dataset shift, enabling more informed decisions about which method to use under which conditions. This line of work could potentially inspire the development of hybrid approaches that leverage insights from related disciplines. While our paper is limited to binary problems, in future work it would also be interesting to investigate extensions of the proposed methods to the multiclass regime.

Acknowledgments

We are grateful to Teodora Popordanoska for her valuable guidance on the LasCal repository. We would also like to thank Andrea Pedrotti for providing code scripts for training language models.

This work has been funded by the QuaDaSh project *Finanziato dall’Unione europea—Next Generation EU, Missione 4 Componente 2 CUP B53D23026250001*.

References

- [Alexandari et al., 2020] Alexandari, A., Kundaje, A., and Shrikumar, A. (2020). Maximum likelihood with bias-corrected calibration is hard-to-beat at label shift adaptation. In *Proceedings of the 37th International Conference on Machine Learning (ICML 2020)*, pages 222–232, Virtual Event.
- [Azizzadenesheli et al., 2019] Azizzadenesheli, K., Liu, A., Yang, F., and Anandkumar, A. (2019). Regularized learning for domain adaptation under label shifts. In *Proceedings of the 7th International Conference on Learning Representations (ICLR 2019)*, New Orleans, US.
- [Barlow and Brunk, 1972] Barlow, R. E. and Brunk, H. D. (1972). The isotonic regression problem and its dual. *Journal of the American Statistical Association*, 67(337):140–147.
- [Beijbom et al., 2015] Beijbom, O., Hoffman, J., Yao, E., Darrell, T., Rodriguez-Ramirez, A., Gonzalez-Rivero, M., and Hoegh-Guldberg, O. (2015). Quantification in-the-wild: Data-sets and baselines. arXiv:1510.04811 [cs.LG].
- [Bella et al., 2010] Bella, A., Ferri, C., Hernández-Orallo, J., and Ramírez-Quintana, M. J. (2010). Quantification via probability estimators. In *Proceedings of the 11th IEEE International Conference on Data Mining (ICDM 2010)*, pages 737–742, Sydney, AU.
- [Benavoli et al., 2016] Benavoli, A., Corani, G., and Mangili, F. (2016). Should we really use post-hoc tests based on mean-ranks? *The Journal of Machine Learning Research*, 17(1):152–161.
- [Bunse, 2022] Bunse, M. (2022). Unification of algorithms for quantification and unfolding. In *Proceedings of the Workshop on Machine Learning for Astroparticle Physics and Astronomy*, pages 459–468, Hamburg, DE.
- [Card and Smith, 2018] Card, D. and Smith, N. A. (2018). The importance of calibration for estimating proportions from annotations. In *Proceedings of the 2018 Conference of the North American Chapter of the Association for Computational Linguistics (HLT-NAACL 2018)*, pages 1636–1646, New Orleans, US.
- [Castaño et al., 2023] Castaño, A., Alonso, J., González, P., and del Coz, J. J. (2023). An equivalence analysis of binary quantification methods. In *Proceedings of the 37th AAAI Conference on Artificial Intelligence (AAAI-23)*, pages 6944–6952, Washington, US.
- [Chen et al., 2021a] Chen, J., Liu, F., Avci, B., Wu, X., Liang, Y., and Jha, S. (2021a). Detecting errors and estimating accuracy on unlabeled data with self-training ensembles. In *Proceedings of the 35th Conference on Neural Information Processing Systems (NeurIPS 2021)*, pages 14980–14992, Virtual Event.
- [Chen and Su, 2023] Chen, J. and Su, B. (2023). Transfer knowledge from head to tail: Uncertainty calibration under long-tailed distribution. In *Proceedings of the IEEE/CVF conference on computer vision and pattern recognition*, pages 19978–19987.
- [Chen et al., 2021b] Chen, M. F., Goel, K., Sohoni, N. S., Poms, F., Fatahalian, K., and Ré, C. (2021b). Mando-line: Model evaluation under distribution shift. In *Proceedings of the 38th International Conference on Machine Learning (ICML 2021)*, pages 1617–1629, Virtual Event.
- [Demšar, 2006] Demšar, J. (2006). Statistical comparisons of classifiers over multiple data sets. *The Journal of Machine learning research*, 7(1):1–30.
- [Devlin et al., 2019] Devlin, J., Chang, M.-W., Lee, K., and Toutanova, K. (2019). BERT: Pre-training of deep bidirectional transformers for language understanding. In *Proceedings of the 2019 conference of the North American chapter of the association for computational linguistics: human language technologies, volume 1 (long and short papers)*, pages 4171–4186.
- [Domingos and Pazzani, 1996] Domingos, P. and Pazzani, M. (1996). Beyond independence: Conditions for the optimality of the simple bayesian classifier. In *Proc. 13th Intl. Conf. Machine Learning*, pages 105–112.
- [du Plessis and Sugiyama, 2012] du Plessis, M. C. and Sugiyama, M. (2012). Semi-supervised learning of class balance under class-prior change by distribution matching. In *Proceedings of the 29th International Conference on Machine Learning (ICML 2012)*, Edinburgh, UK.
- [Dussap et al., 2023] Dussap, B., Blanchard, G., and Chérif-Abdellatif, B. (2023). Label shift quantification with robustness guarantees via distribution feature matching. In *Proceedings of the 34th European Conference on Machine Learning and Principles and Practice of Knowledge Discovery in Databases (ECML / PKDD 2023)*, pages 69–85, Torino, IT.
- [Elkan, 2001] Elkan, C. (2001). The foundations of cost-sensitive learning. In *Proceedings of the 17th International Joint Conference on Artificial Intelligence (IJCAI 2001)*, pages 973–978, Seattle, US.

- [Elsahar and Gallé, 2019] Elsahar, H. and Gallé, M. (2019). To annotate or not? Predicting performance drop under domain shift. In *Proceedings of the 2019 Conference on Empirical Methods in Natural Language Processing and the 9th International Joint Conference on Natural Language Processing (EMNLP-IJCNLP 2019)*, pages 2163–2173, Hong Kong, CN.
- [Esuli et al., 2023] Esuli, A., Fabris, A., Moreo, A., and Sebastiani, F. (2023). *Learning to quantify*. Springer Nature, Cham, CH.
- [Esuli et al., 2021] Esuli, A., Molinari, A., and Sebastiani, F. (2021). A critical reassessment of the Saerens-Latinne-Decaestecker algorithm for posterior probability adjustment. *ACM Transactions on Information Systems*, 39(2):Article 19.
- [Esuli et al., 2022] Esuli, A., Moreo, A., Sebastiani, F., and Sperduti, G. (2022). A detailed overview of LeQua 2022: Learning to quantify. In *Working Notes of the 13th Conference and Labs of the Evaluation Forum (CLEF 2022)*, Bologna, IT.
- [Esuli et al., 2024] Esuli, A., Moreo, A., Sebastiani, F., and Sperduti, G. (2024). An overview of LeQua 2024, the 2nd International Data Challenge on Learning to Quantify. In *Proceedings of the 4th International Workshop on Learning to Quantify (LQ 2024)*, pages 51–78, Vilnius, LT.
- [Esuli and Sebastiani, 2010] Esuli, A. and Sebastiani, F. (2010). Machines that learn how to code open-ended survey data. *International Journal of Market Research*, 52(6):775–800.
- [Fawcett and Flach, 2005] Fawcett, T. and Flach, P. (2005). A response to Webb and Ting’s ‘On the application of ROC analysis to predict classification performance under varying class distributions’. *Machine Learning*, 58(1):33–38.
- [Firat, 2016] Firat, A. (2016). Unified framework for quantification. arXiv:1606.00868v1 [cs.LG] 2 Jun 2016.
- [Flach and Webb, 2016] Flach, Peter A. Eds: Sammut, C. and Webb, G. I. (2016). *Classifier Calibration*, pages 1–8. Springer US, Boston, MA.
- [Forman, 2005] Forman, G. (2005). Counting positives accurately despite inaccurate classification. In *Proceedings of the 16th European Conference on Machine Learning (ECML 2005)*, pages 564–575, Porto, PT.
- [Forman, 2008] Forman, G. (2008). Quantifying counts and costs via classification. *Data Mining and Knowledge Discovery*, 17(2):164–206.
- [Garg et al., 2022] Garg, S., Balakrishnan, S., Lipton, Z. C., Neyshabur, B., and Sedghi, H. (2022). Leveraging unlabeled data to predict out-of-distribution performance. In *Proceedings of the 10th International Conference on Learning Representations (ICLR 2022)*, Virtual Event.
- [Garg et al., 2020] Garg, S., Wu, Y., Balakrishnan, S., and Lipton, Z. (2020). A unified view of label shift estimation. In *Proceedings of the 34th Conference on Neural Information Processing Systems (NeurIPS 2020)*, pages 3290–3300, Virtual Event.
- [Godau et al., 2025] Godau, P., Kalinowski, P., Christodoulou, E., Reinke, A., Tizabi, M., Ferrer, L., Jäger, P., and Maier-Hein, L. (2025). Navigating prevalence shifts in image analysis algorithm deployment. *Medical image analysis*, page 103504.
- [González et al., 2017] González, P., Castaño, A., Chawla, N. V., and del Coz, J. J. (2017). A review on quantification learning. *ACM Computing Surveys*, 50(5):74:1–74:40.
- [González et al., 2024] González, P., Moreo, A., and Sebastiani, F. (2024). Binary quantification and dataset shift: An experimental investigation. *Data Mining and Knowledge Discovery*, 38(4):1670–1712.
- [González-Castro et al., 2013] González-Castro, V., Alaiz-Rodríguez, R., and Alegre, E. (2013). Class distribution estimation based on the Hellinger distance. *Information Sciences*, 218:146–164.
- [Guilbert et al., 2024] Guilbert, T., Caelen, O., Chirita, A., and Saerens, M. (2024). Calibration methods in imbalanced binary classification. *Annals of Mathematics and Artificial Intelligence*, 92(5):1319–1352.
- [Guillory et al., 2021] Guillory, D., Shankar, V., Ebrahimi, S., Darrell, T., and Schmidt, L. (2021). Predicting with confidence on unseen distributions. In *Proceedings of the IEEE/CVF International Conference on Computer Vision (ICCV 2021)*, pages 1134–1144, Montreal, CA.
- [Guo et al., 2017] Guo, C., Pleiss, G., Sun, Y., and Weinberger, K. Q. (2017). On calibration of modern neural networks. In *Proceedings of the 34th International Conference on Machine Learning (ICML 2017)*, pages 1321–1330, Sydney, AU.
- [Hastie et al., 2009] Hastie, T., Tibshirani, R., and Friedman, J. (2009). *The elements of statistical learning: Data mining, inference, and prediction*. Springer, Heidelberg, DE, 2nd edition.

- [Hinton, 2015] Hinton, G. (2015). Distilling the knowledge in a neural network. *arXiv preprint arXiv:1503.02531*.
- [Hopkins and King, 2010] Hopkins, D. J. and King, G. (2010). A method of automated nonparametric content analysis for social science. *American Journal of Political Science*, 54(1):229–247.
- [Jiang et al., 2022] Jiang, Y., Nagarajan, V., Baek, C., and Kolter, J. Z. (2022). Assessing generalization of SGD via disagreement. In *Proceedings of the International Conference on Learning Representations (ICLR 2022)*, Virtual Event.
- [Karandikar et al., 2021] Karandikar, A., Cain, N., Tran, D., Lakshminarayanan, B., Shlens, J., Mozer, M. C., and Roelofs, B. (2021). Soft calibration objectives for neural networks. *Advances in Neural Information Processing Systems*, 34:29768–29779.
- [King and Lu, 2008] King, G. and Lu, Y. (2008). Verbal autopsy methods with multiple causes of death. *Statistical Science*, 23(1):78–91.
- [Kull et al., 2019] Kull, M., Perello Nieto, M., Kängsepp, M., Silva Filho, T., Song, H., and Flach, P. (2019). Beyond temperature scaling: Obtaining well-calibrated multi-class probabilities with dirichlet calibration. *Advances in neural information processing systems*, 32.
- [Kull et al., 2017] Kull, M., Silva Filho, T. M., and Flach, P. (2017). Beyond sigmoids: How to obtain well-calibrated probabilities from binary classifiers with beta calibration. *Electronic Journal of Statistics*, 11:5052–5080.
- [Lipton et al., 2018] Lipton, Z. C., Wang, Y., and Smola, A. J. (2018). Detecting and correcting for label shift with black box predictors. In *Proceedings of the 35th International Conference on Machine Learning (ICML 2018)*, pages 3128–3136, Stockholm, SE.
- [Liu et al., 2019] Liu, Y., Ott, M., Goyal, N., Du, J., Joshi, M., Chen, D., Levy, O., Lewis, M., Zettlemoyer, L., and Stoyanov, V. (2019). RoBERTa: A robustly optimized bert pretraining approach. *arXiv preprint arXiv:1907.11692*.
- [Maas et al., 2011] Maas, A. L., Daly, R. E., Pham, P. T., Huang, D., Ng, A. Y., and Potts, C. (2011). Learning word vectors for sentiment analysis. In *Proceedings of the 49th Annual Meeting of the Association for Computational Linguistics: Human Language Technologies*, pages 142–150, Portland, Oregon, USA. Association for Computational Linguistics.
- [Maletzke et al., 2019] Maletzke, A., Moreira dos Reis, D., Cherman, E., and Batista, G. (2019). DyS: A framework for mixture models in quantification. In *Proceedings of the 33rd AAAI Conference on Artificial Intelligence (AAAI 2019)*, pages 4552–4560, Honolulu, US.
- [Moreo et al., 2021] Moreo, A., Esuli, A., and Sebastiani, F. (2021). QuaPy: A Python-based framework for quantification. In *Proceedings of the 30th ACM International Conference on Knowledge Management (CIKM 2021)*, pages 4534–4543, Gold Coast, AU.
- [Moreo et al., 2025] Moreo, A., González, P., and del Coz, J. J. (2025). Kernel density estimation for multiclass quantification. *Machine Learning*, 114(4).
- [Moreo and Sebastiani, 2022] Moreo, A. and Sebastiani, F. (2022). Tweet sentiment quantification: An experimental re-evaluation. *PLOS ONE*, 17(9):1–23.
- [Murphy, 1972] Murphy, A. H. (1972). Scalar and vector partitions of the probability score: Part i. two-state situation. *Journal of Applied Meteorology and Climatology*, 11(2):273–282.
- [Ovadia et al., 2019] Ovadia, Y., Fertig, E., Ren, J., Nado, Z., Sculley, D., Nowozin, S., Dillon, J., Lakshminarayanan, B., and Snoek, J. (2019). Can you trust your model’s uncertainty? evaluating predictive uncertainty under dataset shift. *Advances in neural information processing systems*, 32.
- [Pang and Lee, 2005] Pang, B. and Lee, L. (2005). Seeing stars: Exploiting class relationships for sentiment categorization with respect to rating scales. In *Proceedings of the 43rd Annual Meeting of the Association for Computational Linguistics (ACL’05)*, pages 115–124.
- [Park et al., 2020] Park, S., Bastani, O., Weimer, J., and Lee, I. (2020). Calibrated prediction with covariate shift via unsupervised domain adaptation. In *International Conference on Artificial Intelligence and Statistics*, pages 3219–3229. PMLR.
- [Patrone and Kearsley, 2024] Patrone, P. N. and Kearsley, A. J. (2024). Minimizing uncertainty in prevalence estimates. *Statistics & Probability Letters*, 205:109946.
- [Pedregosa et al., 2011] Pedregosa, F., Varoquaux, G., Gramfort, A., Michel, V., Thirion, B., Grisel, O., Blondel, M., Prettenhofer, P., Weiss, R., Dubourg, V., Vanderplas, J., Passos, A., Cournapeau, D., Brucher, M., Perrot, M., and Duchesnay, E. (2011). Scikit-learn: Machine learning in Python. *Journal of Machine Learning Research*, 12:2825–2830.

- [Platt, 2000] Platt, J. C. (2000). Probabilistic outputs for support vector machines and comparison to regularized likelihood methods. In Smola, A., Bartlett, P., Schölkopf, B., and Schuurmans, D., editors, *Advances in Large Margin Classifiers*, pages 61–74. The MIT Press, Cambridge, MA.
- [Popordanoska et al., 2024] Popordanoska, T., Radevski, G., Tuytelaars, T., and Blaschko, M. (2024). Lascal: Label-shift calibration without target labels. *Proceedings NeurIPS 2024*.
- [Pérez-Gállego et al., 2017] Pérez-Gállego, P., Quevedo, J. R., and del Coz, J. J. (2017). Using ensembles for problems with characterizable changes in data distribution: A case study on quantification. *Information Fusion*, 34:87–100.
- [Pérez-Mon et al., 2025] Pérez-Mon, O., Moreo, A., del Coz, J. J., and González, P. (2025). Quantification using permutation-invariant networks based on histograms. *Neural Computing and Applications*, 37:3505–3520.
- [Rabanser et al., 2019] Rabanser, S., Günnemann, S., and Lipton, Z. C. (2019). Failing loudly: An empirical study of methods for detecting dataset shift. In *Proceedings of the 33rd Conference on Neural Information Processing Systems (NeurIPS 2019)*, pages 1394–1406, Vancouver, CA.
- [Saerens et al., 2002] Saerens, M., Latinne, P., and Decaestecker, C. (2002). Adjusting the outputs of a classifier to new a priori probabilities: A simple procedure. *Neural Computation*, 14(1):21–41.
- [Sanh et al., 2019] Sanh, V., Debut, L., Chaumond, J., and Wolf, T. (2019). DistilBERT, a distilled version of BERT: smaller, faster, cheaper and lighter. *arXiv preprint arXiv:1910.01108*.
- [Schumacher et al., 2025] Schumacher, T., Strohmaier, M., and Lemmerich, F. (2025). A comparative evaluation of quantification methods. *Journal of Machine Learning Research*, 26(55):1–54.
- [Sebastiani, 2020] Sebastiani, F. (2020). Evaluation measures for quantification: An axiomatic approach. *Information Retrieval Journal*, 23(3):255–288.
- [Silva Filho et al., 2023] Silva Filho, T., Song, H., Perello-Nieto, M., Santos-Rodriguez, R., Kull, M., and Flach, P. (2023). Classifier calibration: a survey on how to assess and improve predicted class probabilities. *Machine Learning*, 112(9):3211–3260.
- [Storkey, 2009] Storkey, A. (2009). When training and test sets are different: Characterizing learning transfer. In Quiñero-Candela, J., Sugiyama, M., Schwaighofer, A., and Lawrence, N. D., editors, *Dataset shift in machine learning*, pages 3–28. The MIT Press, Cambridge, US.
- [Tasche, 2014] Tasche, D. (2014). 4.12 classification, calibration, and quantification: A study of dataset shift. *Beyond Adaptation: Understanding Distributional Changes*, 7(4):28.
- [Tasche, 2021] Tasche, D. (2021). Calibrating sufficiently. *Statistics*, 55(6):1356–1386.
- [Tasche, 2022] Tasche, D. (2022). Class prior estimation under covariate shift: No problem? In *Proceedings of the 2nd International Workshop on Learning to Quantify (LQ 2022)*, pages 11–26, Grenoble, IT.
- [Tasche, 2023] Tasche, D. (2023). Invariance assumptions for class distribution estimation. In *Proceedings of the 3rd International Workshop on Learning to Quantify (LQ 2023)*, pages 56–71, Torino, IT.
- [Volpi et al., 2024] Volpi, L., Moreo, A., and Sebastiani, F. (2024). A simple method for classifier accuracy prediction under prior probability shift. In *Proceedings of the 27th International Conference on Discovery Science (DS 2024)*, pages 267–283, Pisa, IT.
- [Wang et al., 2020] Wang, X., Long, M., Wang, J., and Jordan, M. (2020). Transferable calibration with lower bias and variance in domain adaptation. In Larochelle, H., Ranzato, M., Hadsell, R., Balcan, M., and Lin, H., editors, *Advances in Neural Information Processing Systems*, volume 33, pages 19212–19223. Curran Associates, Inc.
- [Wu and Resnick, 2024] Wu, S. and Resnick, P. (2024). Calibrate-extrapolate: Rethinking prevalence estimation with black box classifiers.
- [Zadrozny and Elkan, 2001a] Zadrozny, B. and Elkan, C. (2001a). Obtaining calibrated probability estimates from decision trees and naive bayesian classifiers. In *ICML*, volume 1, pages 609–616.
- [Zadrozny and Elkan, 2001b] Zadrozny, B. and Elkan, C. (2001b). Obtaining calibrated probability estimates from decision trees and naive Bayesian classifiers. In *Proceedings of the 18th International Conference on Machine Learning (ICML 2001)*, pages 609–616, Williamstown, US.
- [Zhang et al., 2015] Zhang, X., Zhao, J., and LeCun, Y. (2015). Character-level convolutional networks for text classification. *Advances in neural information processing systems*, 28.

A Classifiers accuracy

Table 8 reports the classifiers accuracy of different LM models on the sentiment datasets, for different combinations of source and target domains, while Table 9 reports the accuracy of our classifiers of choice for the tabular datasets in the UCI Machine Learning repository.

Table 8: LM’s accuracy on sentiment classification datasets

	source	target		
		imdb	rt	yelp
BERT	imdb	0.751	0.689	0.734
	rt	0.697	0.689	0.694
	yelp	0.730	0.702	0.889
DistilBERT	imdb	0.855	0.773	0.865
	rt	0.823	0.785	0.809
	yelp	0.772	0.713	0.909
RoBERTa	imdb	0.848	0.695	0.865
	rt	0.732	0.737	0.749
	yelp	0.844	0.735	0.940

Table 9: Classifiers accuracy on UCI Machine Learning datasets

	Logistic Regression	Multi-layer Perceptron	Naïve Bayes	k Nearest Neighbor
cmc.3	0.663	0.683	0.649	0.667
ctg.1	0.918	0.933	0.897	0.911
ctg.2	0.918	0.920	0.743	0.908
ctg.3	0.972	0.969	0.958	0.955
pageblocks.5	0.981	0.986	0.976	0.982
semeion	0.962	0.969	0.793	0.964
spambase	0.927	0.935	0.826	0.896
wine-q-red	0.758	0.781	0.742	0.723
wine-q-white	0.739	0.763	0.684	0.761
yeast	0.771	0.769	0.300	0.749

B Brier Scores in calibration experiments

Tables 10 and 11 report the Brier Scores obtained in our calibration experiments for CS and LS, respectively. The Brier Score (BS) is defined as:

$$\text{BS} = \frac{1}{|D_{te}|} \sum_{(x_i, y_i) \in D_{te}} (y_i - \tilde{h}(x_i))^2 \quad (34)$$

where $y_i \in \{0, 1\}$ is the true label of the i -th test instance, and $\tilde{h}(x_i)$ is its predicted posterior probability, as estimated by a calibrated classifier \tilde{h} .

Table 10: Calibration performance under CS in terms of Brier Score

		Baselines		Reference				Adapted Methods													
		Platt	Head2Tail	CPCS	TransCal	LasCal	PCC ^{EB} _{0.25}	PACC ^{EB} _{0.25}	EMQ ^{EB} _{0.25}	KDEy ^{EB} _{0.25}	ATC ^{EB} _{0.25}	Doc ^{EB} _{0.25}	LEAP ^{EB} _{0.25}	LEAP ^{PCC-EB} _{0.25}	EMQ	EMQ ^{ECTS}	EMQ ^{TransCal}	PacCal ^r	DMCal		
BERT	imdb→rt	0.188	0.206	0.214	0.197	0.187	0.188	0.189	0.202	0.210	0.188	0.185	0.191	0.204	0.230	0.216	0.362	0.188	0.214		
	imdb→yelp	0.169	0.199	0.199	0.189	0.173	0.177	0.171	0.179	0.175	0.172	0.173	0.189	0.206	0.203	0.221	0.235	0.170	0.176		
	rt→imdb	0.197	0.238	0.233	0.218	0.199	0.207	0.197	0.218	0.209	0.200	0.202	0.200	0.224	0.508	0.384	0.508	0.209	0.249		
	rt→yelp	0.202	0.239	0.238	0.221	0.203	0.211	0.203	0.211	0.225	0.202	0.205	0.208	0.231	0.500	0.236	0.500	0.215	0.229		
	yelp→imdb	0.138	0.132	0.154	0.133	0.156	0.132	0.136	0.153	0.167	0.132	0.134	0.154	0.154	0.167	0.163	0.214	0.140	0.162		
	yelp→rt	0.154	0.146	0.173	0.148	0.184	0.146	0.151	0.163	0.176	0.152	0.148	0.171	0.167	0.174	0.172	0.211	0.152	0.171		
DistiBERT	imdb→rt	0.136	0.133	0.142	0.137	0.147	0.132	0.136	0.147	0.150	0.170	0.133	0.146	0.135	0.138	0.136	0.154	0.137	0.136		
	imdb→yelp	0.100	0.102	0.106	0.103	0.108	0.100	0.099	0.106	0.106	0.123	0.099	0.106	0.101	0.100	0.099	0.120	0.111	0.099		
	rt→imdb	0.139	0.164	0.153	0.145	0.142	0.141	0.143	0.155	0.147	0.154	0.140	0.165	0.157	0.442	0.143	0.508	0.142	0.143		
	rt→yelp	0.141	0.159	0.163	0.145	0.147	0.141	0.148	0.162	0.145	0.145	0.142	0.165	0.165	0.434	0.161	0.500	0.142	0.159		
	yelp→imdb	0.117	0.113	0.121	0.114	0.145	0.113	0.114	0.128	0.118	0.114	0.113	0.133	0.133	0.137	0.128	0.164	0.128	0.126		
	yelp→rt	0.140	0.131	0.144	0.131	0.175	0.132	0.135	0.150	0.144	0.146	0.132	0.157	0.149	0.147	0.141	0.161	0.142	0.140		
RoBERTa	imdb→rt	0.162	0.157	0.177	0.159	0.179	0.157	0.164	0.182	0.181	0.206	0.159	0.172	0.153	0.194	0.192	0.239	0.159	0.187		
	imdb→yelp	0.102	0.104	0.122	0.108	0.104	0.104	0.102	0.109	0.109	0.116	0.102	0.107	0.107	0.102	0.102	0.122	0.112	0.102		
	rt→imdb	0.177	0.178	0.191	0.182	0.186	0.178	0.184	0.202	0.175	0.178	0.178	0.204	0.212	0.504	0.225	0.508	0.182	0.207		
	rt→yelp	0.171	0.174	0.189	0.181	0.176	0.174	0.177	0.188	0.171	0.173	0.173	0.196	0.206	0.496	0.219	0.500	0.175	0.202		
	yelp→imdb	0.082	0.077	0.078	0.077	0.099	0.078	0.078	0.082	0.093	0.079	0.078	0.086	0.086	0.082	0.086	0.098	0.110	0.085		
	yelp→rt	0.116	0.110	0.113	0.109	0.147	0.109	0.110	0.122	0.119	0.135	0.111	0.123	0.111	0.111	0.111	0.124	0.135	0.111		
Wins	Pr(M > 1R)	†96.83%	—	—	—	—	†99.17%	†95.00%	75.28%	79.89%	79.22%	†99.78%	75.00%	73.56%	52.17%	72.17%	27.00%	80.28%	80.61%		
	Pr(M > 2R)	†73.61%	—	—	—	—	†86.11%	†74.94%	41.17%	44.17%	54.33%	†92.50%	34.56%	35.83%	30.94%	45.89%	4.94%	54.17%	51.06%		
	Pr(M > 3R)	†51.89%	—	—	—	—	†60.89%	†47.17%	24.33%	28.28%	39.33%	†61.33%	18.72%	17.06%	26.06%	0.61%	32.56%	29.11%			
	Pr(M > 4R)	†36.61%	—	—	—	—	†23.89%	†28.56%	12.67%	17.33%	25.89%	†26.94%	5.83%	10.28%	7.94%	13.17%	0.22%	15.72%	17.17%		
Ave Rank		5.89	8.37	9.90	7.25	9.55	5.94	6.18	10.92	10.81	9.30	4.99	11.81	11.47	12.57	10.35	16.86	9.67	9.19		

Table 11: Calibration performance under label shift in terms of Brier Score

		Baselines				Reference				Adapted Methods													
		Platt	Head2Tail	CPCS	TransCal	LasCal	PACC ^{EB} _{0.25}	EMQ ^{EB} _{0.25}	KDEy ^{EB} _{0.25}	ATC ^{EB} _{0.25}	Doc ^{EB} _{0.25}	LEA ^{EB} _{0.25}	EMQ	EMQ ^{ECTS}	EMQ ^{LasCal}	PacCal ^r	DMCal						
Logistic Regression	cmc.3	0.248	0.242	0.241	0.243	0.240	0.240	0.244	0.231	0.274	0.252	0.240	0.177	0.173	0.261	0.309	0.177						
	yeast	0.215	0.217	0.198	0.200	0.194	0.187	0.182	0.195	0.192	0.197	0.198	0.150	0.142	0.242	0.196	0.135						
	semeion	0.108	0.107	0.117	0.089	0.101	0.069	0.057	0.060	0.091	0.073	0.085	0.036	0.030	0.098	0.107	0.048						
	wine-q-red	0.175	0.186	0.176	0.178	0.177	0.175	0.189	0.191	0.218	0.175	0.173	0.128	0.128	0.128	0.176	0.128						
	ctg.1	0.098	0.093	0.093	0.093	0.094	0.075	0.085	0.083	0.147	0.103	0.087	0.055	0.055	0.061	0.099	0.058						
	ctg.2	0.161	0.138	0.138	0.138	0.156	0.079	0.082	0.081	0.099	0.106	0.105	0.061	0.077	0.217	0.094	0.060						
	ctg.3	0.098	0.105	0.104	0.096	0.096	0.070	0.051	0.053	0.061	0.056	0.074	0.034	0.034	0.081	0.105	0.041						
	spambase	0.059	0.058	0.058	0.061	0.058	0.058	0.056	0.055	0.058	0.059	0.056	0.047	0.047	0.059	0.091	0.045						
	wine-q-white	0.219	0.216	0.212	0.215	0.204	0.205	0.217	0.218	0.266	0.290	0.209	0.135	0.134	0.174	0.203	0.136						
	pageblocks.5	0.276	0.300	0.337	0.224	0.178	0.132	0.089	0.116	0.124	0.116	0.140	0.055	0.055	0.404	0.141	0.083						
Naive Bayes	cmc.3	0.239	0.225	0.222	0.229	0.218	0.236	0.236	0.236	0.226	0.239	0.234	0.175	0.174	0.211	0.294	0.181						
	yeast	0.283	0.255	0.249	0.522	0.286	0.497	0.496	0.496	0.522	0.522	0.522	0.523	0.523	0.519	0.390	0.522						
	semeion	0.286	0.161	0.186	0.200	0.166	0.187	0.185	0.186	0.201	0.201	0.201	0.201	0.201	0.201	0.160	0.201						
	wine-q-red	0.189	0.208	0.191	0.221	0.192	0.190	0.184	0.190	0.269	0.203	0.225	0.172	0.185	0.152	0.200	0.154						
	ctg.1	0.141	0.145	0.119	0.106	0.119	0.091	0.091	0.091	0.174	0.170	0.105	0.094	0.067	0.139	0.117	0.090						
	ctg.2	0.246	0.172	0.178	0.162	0.160	0.165	0.169	0.167	0.201	0.202	0.187	0.195	0.195	0.294	0.154	0.180						
	ctg.3	0.186	0.146	0.146	0.155	0.136	0.149	0.149	0.144	0.153	0.153	0.169	0.151	0.151	0.250	0.127	0.152						
	spambase	0.127	0.134	0.132	0.156	0.140	0.153	0.154	0.153	0.158	0.158	0.157	0.157	0.157	0.129	0.129	0.156						
	wine-q-white	0.245	0.221	0.221	0.218	0.221	0.218	0.228	0.225	0.358	0.296	0.256	0.216	0.149	0.210	0.256	0.176						
	pageblocks.5	0.323	0.276	0.255	0.218	0.177	0.185	0.130	0.143	0.190	0.199	0.228	0.107	0.107	0.256	0.176	0.175						
k Nearest Neighbor	cmc.3	0.248	0.237	0.237	0.236	0.223	0.257	0.257	0.257	0.329	0.273	0.250	0.191	0.192	0.246	0.323	0.194						
	yeast	0.214	0.212	0.195	0.196	0.208	0.202	0.204	0.203	0.212	0.215	0.202	0.143	0.143	0.196	0.205	0.136						
	semeion	0.051	0.094	0.100	0.105	0.094	0.048	0.040	0.040	0.137	0.097	0.075	0.032	0.032	0.029	0.092	0.027						
	wine-q-red	0.191	0.200	0.192	0.199	0.194	0.200	0.203	0.203	0.205	0.194	0.202	0.144	0.144	0.140	0.199	0.138						
	ctg.1	0.107	0.118	0.115	0.111	0.121	0.087	0.082	0.082	0.109	0.137	0.084	0.054	0.054	0.057	0.106	0.055						
	ctg.2	0.152	0.146	0.143	0.132	0.166	0.086	0.081	0.081	0.210	0.083	0.090	0.056	0.056	0.066	0.102	0.057						
	ctg.3	0.122	0.162	0.175	0.114	0.133	0.089	0.051	0.051	0.105	0.078	0.098	0.035	0.035	0.037	0.116	0.041						
	spambase	0.083	0.084	0.085	0.097	0.085	0.081	0.084	0.084	0.098	0.082	0.096	0.062	0.062	0.062	0.102	0.061						
	wine-q-white	0.208	0.204	0.200	0.206	0.196	0.195	0.209	0.209	0.321	0.217	0.204	0.149	0.149	0.140	0.188	0.141						
	pageblocks.5	0.235	0.272	0.250	0.210	0.179	0.149	0.131	0.133	0.209	0.146	0.152	0.113	0.113	0.116	0.138	0.124						
Multi-layer Perceptron	cmc.3	0.232	0.227	0.225	0.229	0.213	0.227	0.223	0.235	0.256	0.255	0.240	0.170	0.156	0.257	0.271	0.159						
	yeast	0.219	0.202	0.196	0.198	0.194	0.187	0.188	0.192	0.214	0.211	0.207	0.150	0.140	0.217	0.202	0.144						
	semeion	0.063	0.066	0.074	0.061	0.060	0.048	0.041	0.044	0.025	0.030	0.033	0.023	0.024	0.081	0.091	0.022						
	wine-q-red	0.170	0.178	0.171	0.171	0.171	0.171	0.179	0.179	0.229	0.172	0.195	0.132	0.125	0.125	0.171	0.129						
	ctg.1	0.088	0.082	0.083	0.082	0.084	0.067	0.063	0.064	0.137	0.105	0.068	0.046	0.043	0.092	0.096	0.049						
	ctg.2	0.157	0.131	0.138	0.139	0.140	0.070	0.072	0.070	0.101	0.080	0.109	0.058	0.066	0.168	0.101	0.060						
	ctg.3	0.098	0.106	0.106	0.093	0.095	0.066	0.051	0.052	0.081	0.078	0.072	0.034	0.033	0.119	0.105	0.049						
	spambase	0.054	0.051	0.050	0.050	0.050	0.049	0.049	0.048	0.058	0.048	0.052	0.041	0.038	0.062	0.088	0.042						
	wine-q-white	0.193	0.189	0.188	0.190	0.184	0.186	0.196	0.196	0.263	0.212	0.193	0.125	0.123	0.152	0.176	0.124						
	pageblocks.5	0.190	0.186	0.206	0.146	0.141	0.146	0.076	0.082	0.122	0.099	0.127	0.041	0.041	0.248	0.120	0.060						
Wins	Pr(M > 1R)	65.65%	—	—	—	—	76.53%	70.25%	70.30%	52.83%	64.70%	66.83%	†86.42%	†87.25%	61.50%	57.85%	†89.70%						
	Pr(M > 2R)	48.30%	—	—	—	—	64.03%	59.50%	59.77%	45.07%	54.30%	57.10%	†77.98%	†79.38%	51.30%	49.90%	†81.95%						
	Pr(M > 3R)	35.65%	—	—	—	—	58.73%	55.77%	56.07%	41.10%	47.23%	52.50%	†73.80%	†75.95%	46.85%	45.75%	†76.98%						
	Pr(M > 4R)	26.70%	—	—	—	—	52.18%	50.85%	50.88%	34.85%	42.33%	45.30%	†69.00%	†71.65%	44.07%	39.07%	†72.02%						
Ave Rank		10.22	10.14	9.48	9.83	8.99	8.07	7.84	8.15	10.82	9.57	9.57	4.97	4.61	8.79	10.55	4.40						